



institut
universitaire
de France



SORBONNE
UNIVERSITÉ

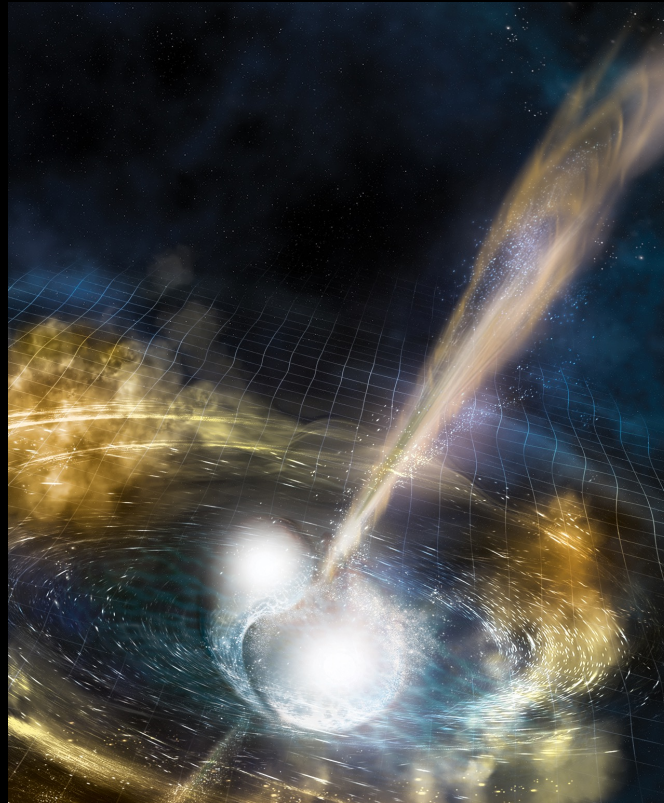


MULTI-MESSENGER THEORY AND MODELLING

(WITH A STRONG FOCUS ON BNS AND GRAVITATIONAL WAVES)

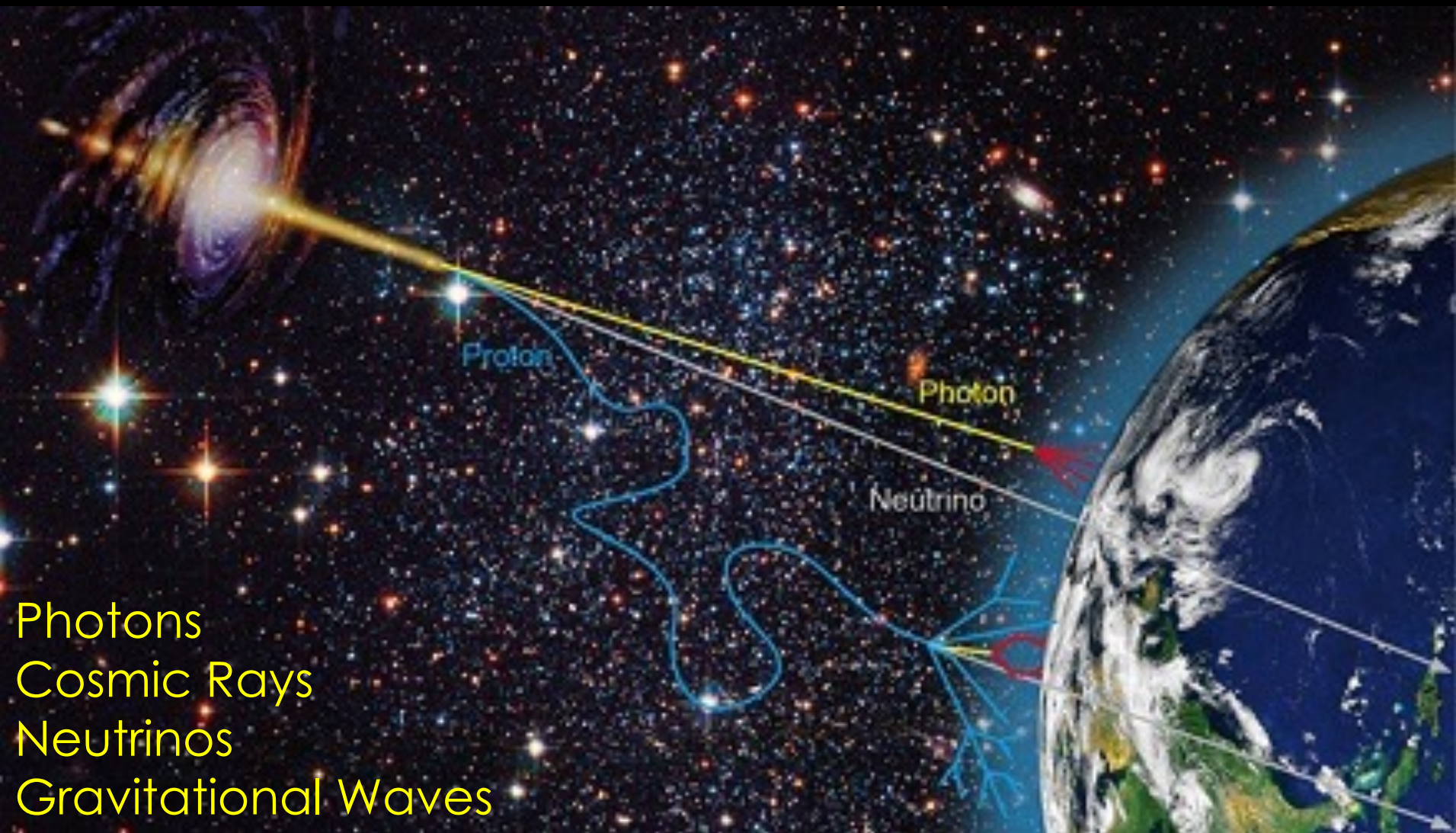
Frédéric Daigne

(Institut d'Astrophysique de Paris; Sorbonne University)



Multi-Messenger Astrophysics

Multi-Messenger Astrophysics



Neutrinos

Neutrinos (1) Solar Neutrinos

- Nuclear fusion: $4p + 2e^- \rightarrow \frac{4}{2} \text{He} + 2\nu_e + 26.7 \text{ MeV}$
Neutrinos carry ~2% of the energy released ($\langle E_\nu \rangle = 0.26 \text{ MeV}$)

- **Neutrino flux from the Sun: $6.6 \cdot 10^{10} \nu/\text{s}/\text{cm}^2$**

- **Detailed prediction of the neutrino spectrum (Bahcall)**

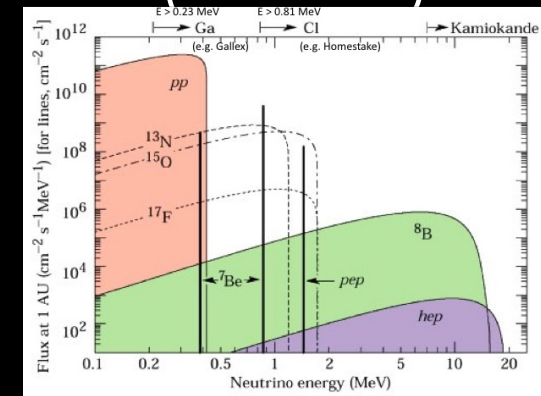
- **Many experiments**

Homestake 1970-1994 ; Gallex 1991-1997



Kamiokande/Super-K 1993- Elastic scattering / beta decay

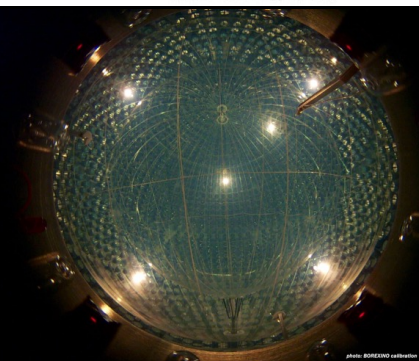
Borexino (Gran Sasso) 2007- Organic liquid scintillator



- **Two major results:**

- **Astrophysics: confirmation of the source of energy of the Sun (hydrogen nuclear burning)**

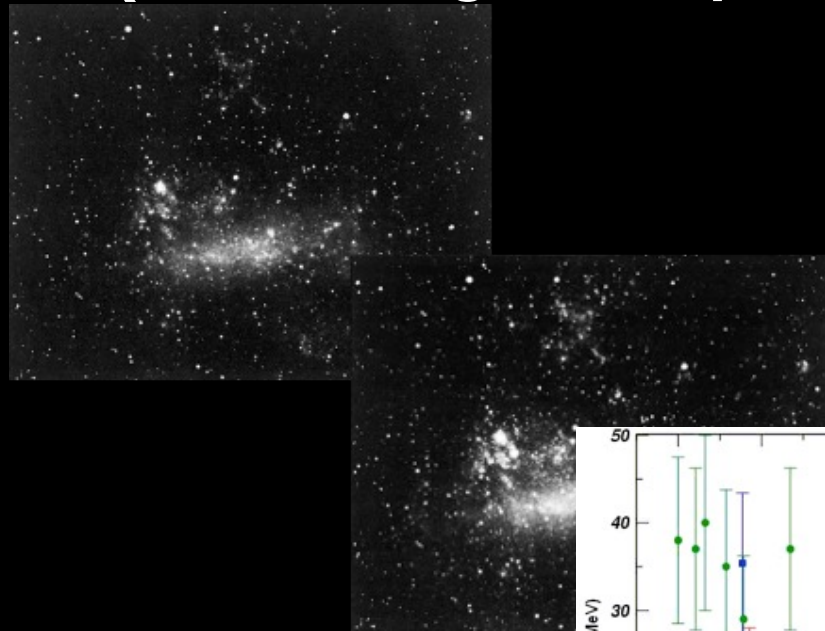
- **Fundamental physics: neutrino oscillation (BSM)**



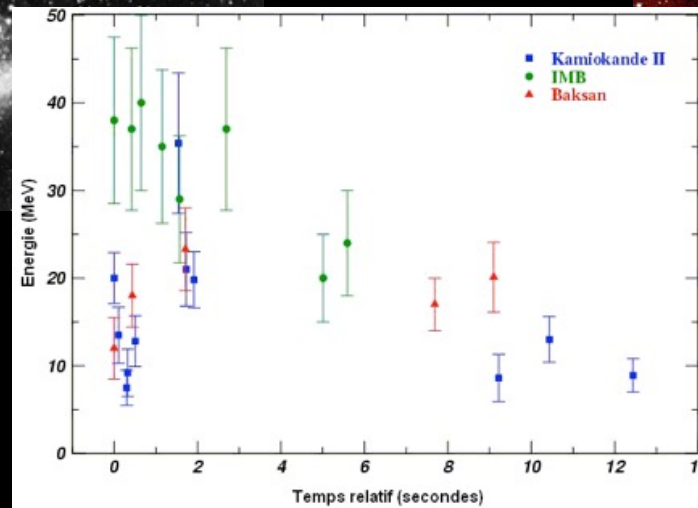
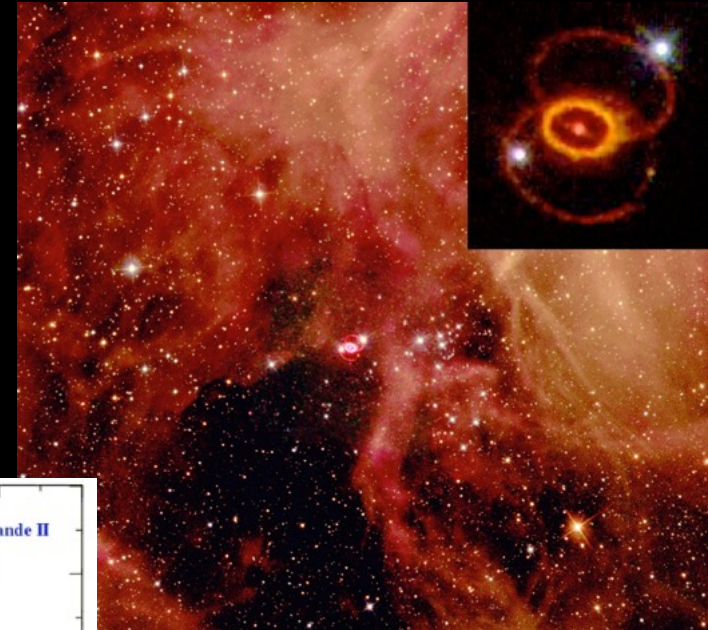
Neutrinos (2) SN1987A in LMC

Two major results:

- Astrophysics: validation of the core-collapse scenario
- Fundamental physics: limit on neutrino mass (neutrino-light delay $\sim 3h$)



HST

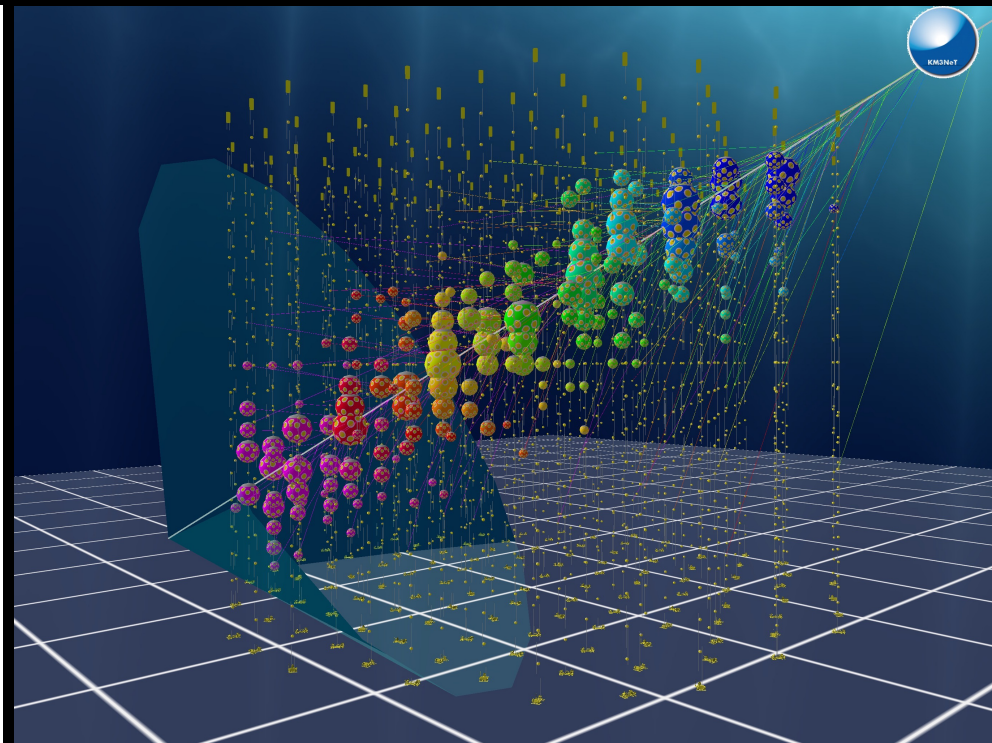
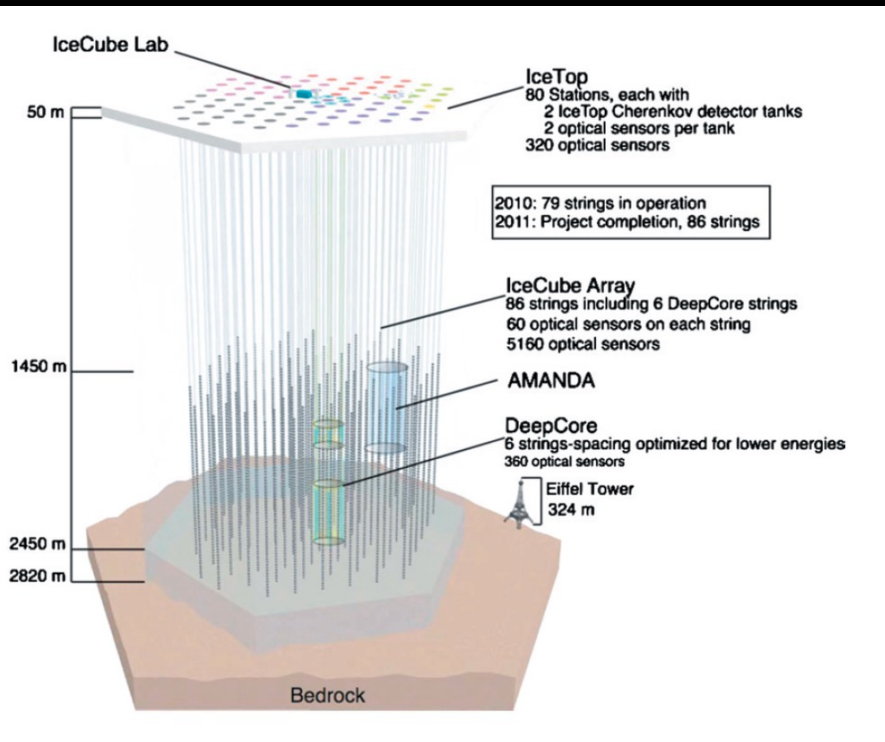


Kamiokande: $12\bar{\nu}_e$ in 13 s
Total energy released in neutrinos: $\sim 10^{53}$ erg
 $\sim G M_{NS}^2 / R_{NS}$

Neutrinos (3) High-energy neutrinos

Technique = muon production, Cerenkov light (ice, water)

- IceCube: Antarctica
- ANTARES → KM3NET: Mediterranean Sea



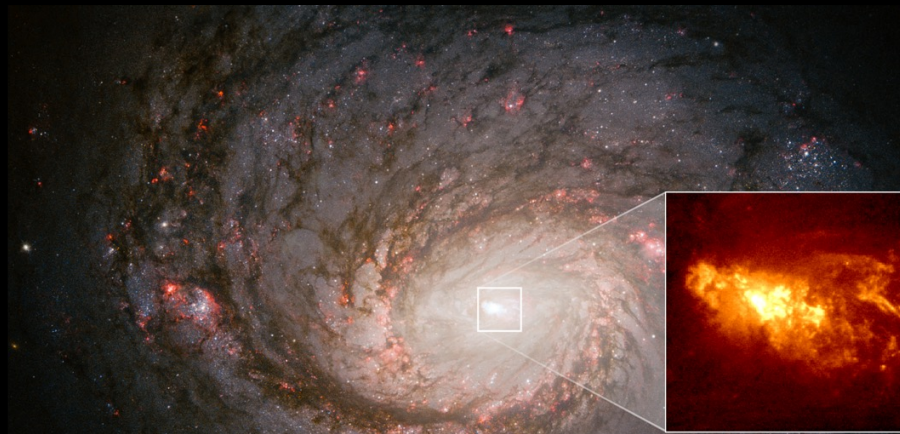
Neutrinos (3) High-energy neutrinos

Detections by IceCube

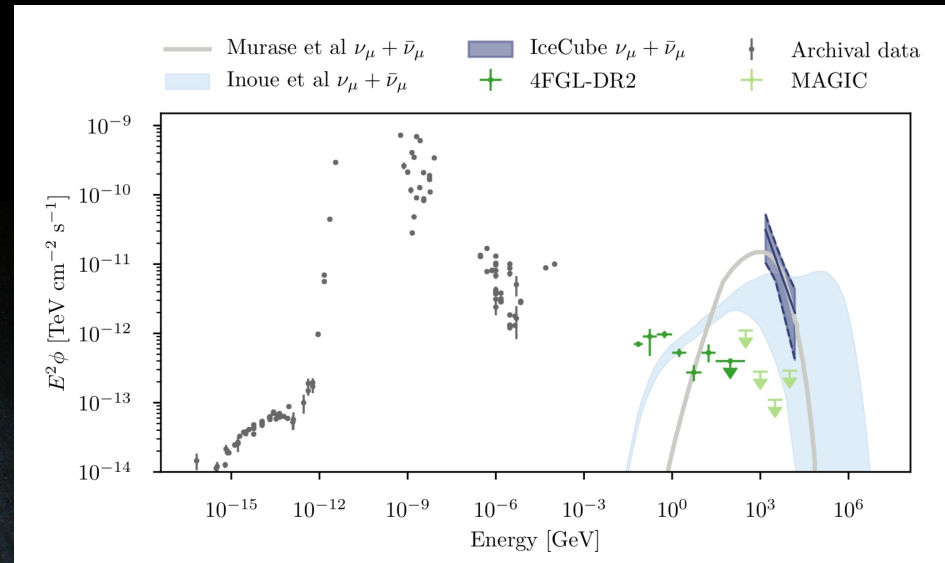
- Quasi-isotropic diffuse background (10 TeV to a few PeV) (Aartsen+ 2013)
- Space & time coincidence of a HE ν with γ -ray flaring blazar TXS 0506+056 (Aartsen+ 2018)
- Possible detection (4.2σ): active galaxy NGC1068 =M77 (Abbasi+ 2022)

Advances on particle acceleration are expected.

HE neutrino production: $p\gamma$ or pp



HST: NGC 1608



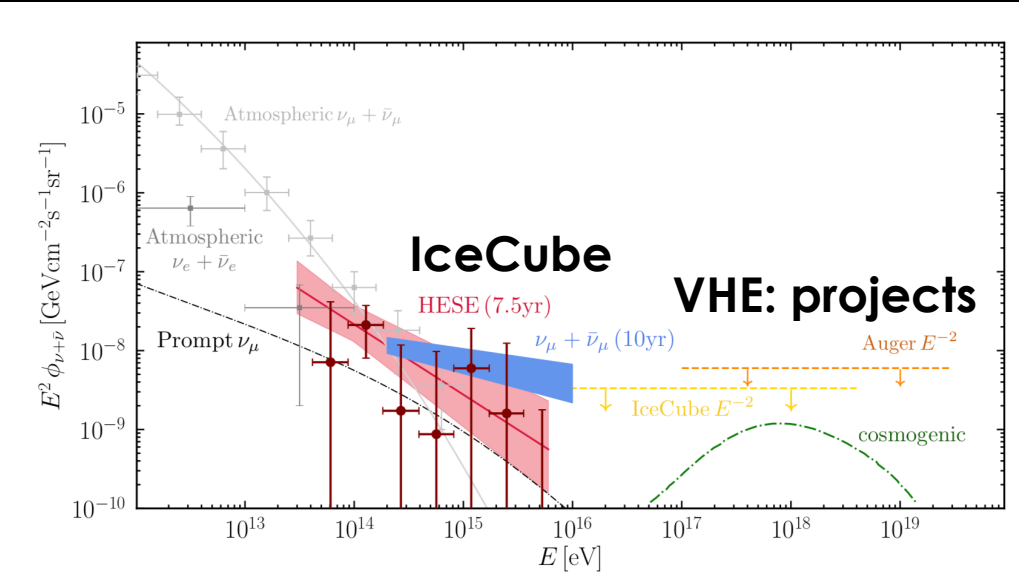
(Abbasi+ 2022)

Model: disk+corona
 $p\gamma$ interactions

Neutrinos (4) Diffuse background

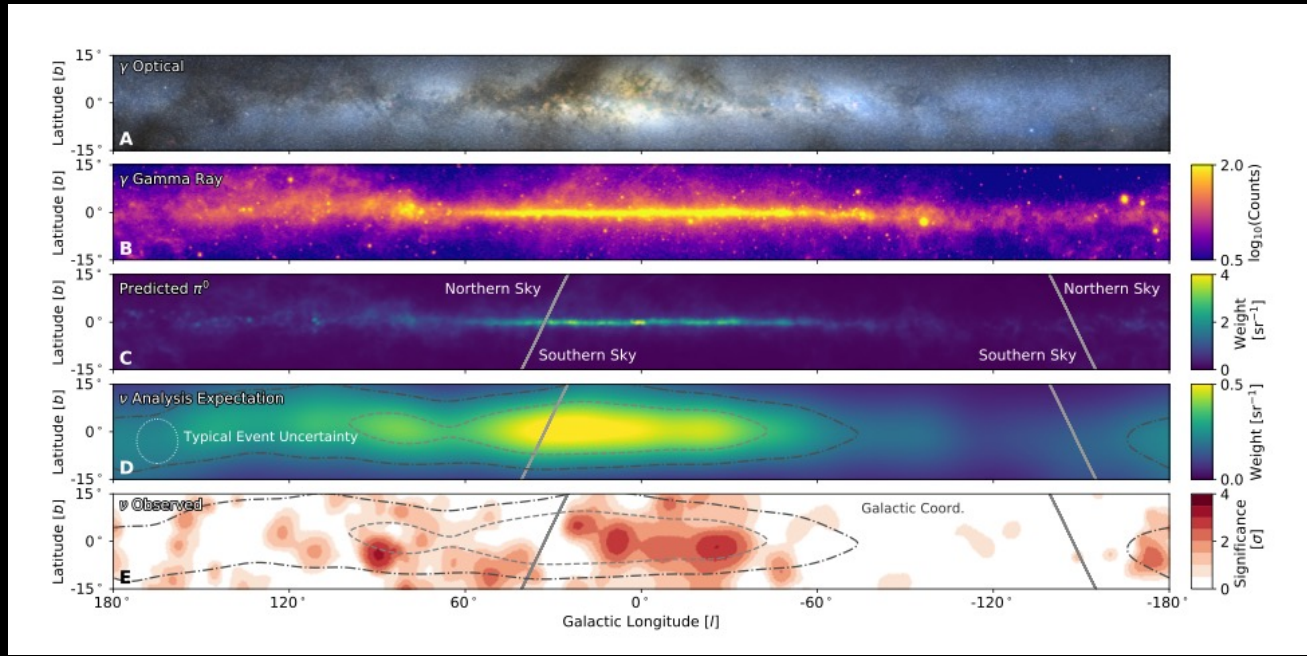
- High-energy: already detected by IceCube

Sources?
 (a dominant class or several?)
 Candidates: AGNs, GRBs, etc.)



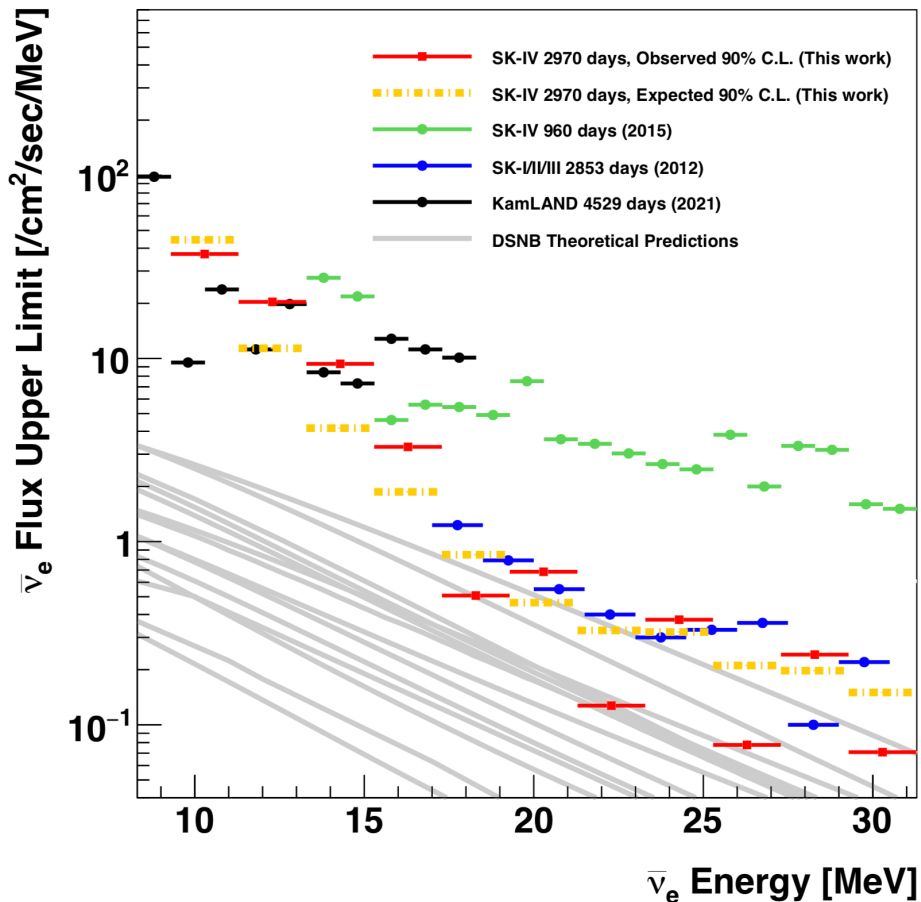
Diffuse HE neutrino emission from the Galactic plane?

detection by IceCube at 4.5σ



Neutrinos (4) Diffuse background

- High-energy: already detected by IceCube
- MeV: Diffuse Astrophysical Neutrino Background to be detected soon?
= DSNB dominated by unresolved core-collapse supernovae



DSNB search with super-K
(Abe+ 2022)
Analysis for 22.5 x 8.1 kton-year

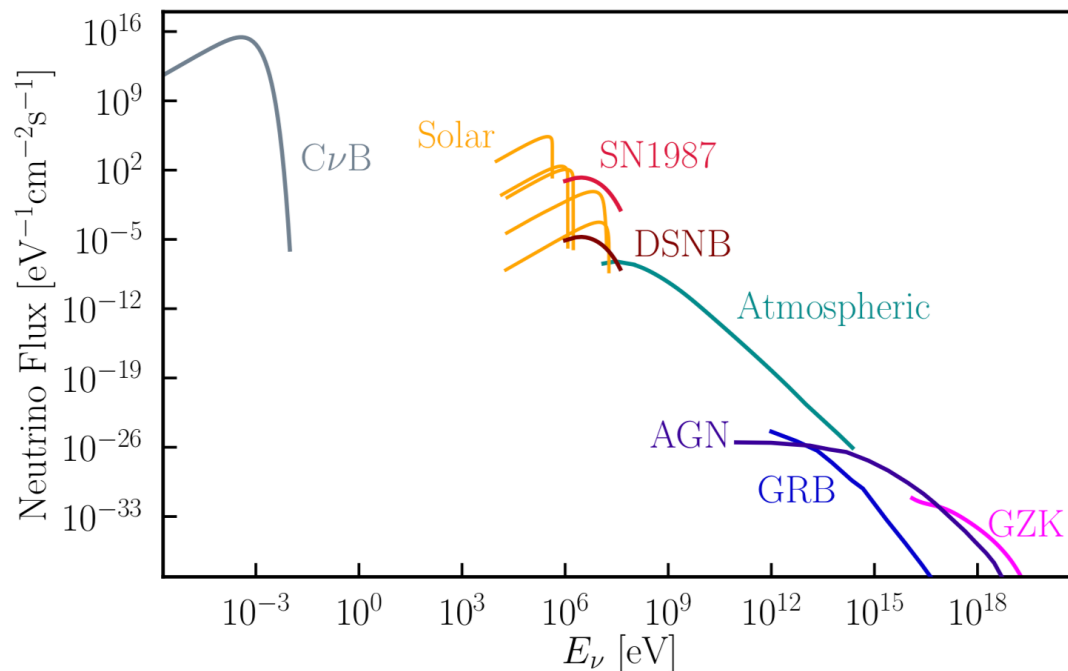
Super-K close to detection?
Hyper-K?

Gray: DSNB models differ on:

- cosmic SFR
- cc physics (failed SNe, ...)
- ν physics (flavor conversion, ..)

Neutrinos (4) Diffuse background

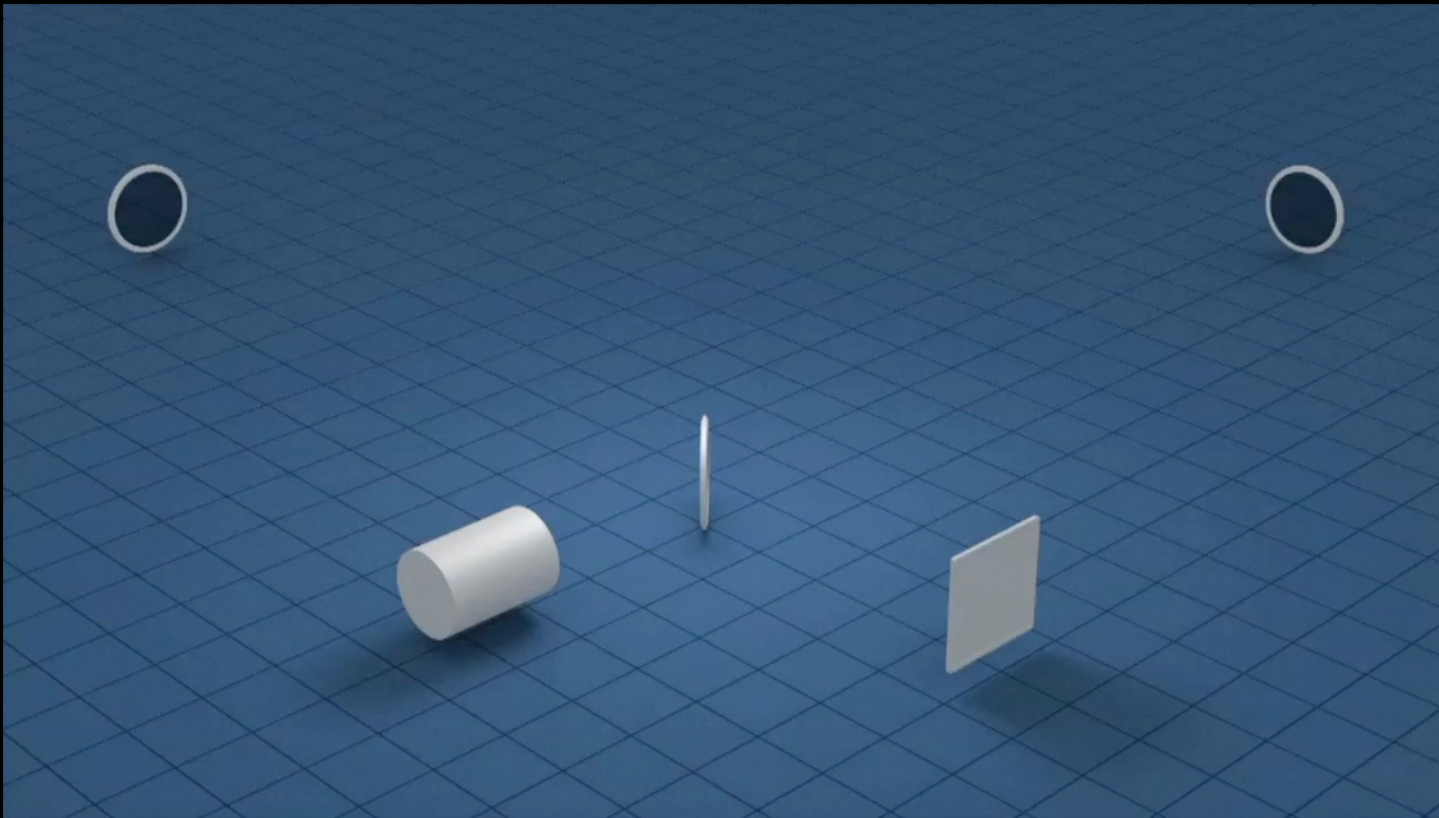
- High-energy: already detected by IceCube
- MeV: Diffuse Astrophysical Neutrino Background to be detected soon?
= DSNB dominated by unresolved core-collapse supernovae
- **Primordial neutrino background:**
 - **Decoupling at ~ 1 s after the Big Bang**
 - **$T_{\text{C}\nu\text{B},0} \sim 1.95$ K: unthinkable detection with present or potential techniques**



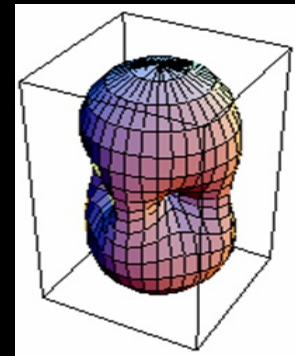
Gravitational Waves

Detection

- Direction-dependent variation of length: interferometers



- Typical strain from a stellar-mass binary: $h \sim 10^{-21}$
- Sensitivity of the interferometer depends on direction and polarization state



Detection: Hz-kHz

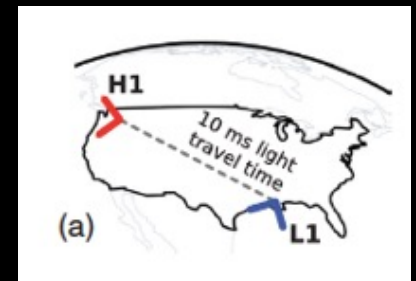
- Hz-kHz: ground-based interferometric detectors
Ligo-Virgo-Kagra



Virgo (3 km)

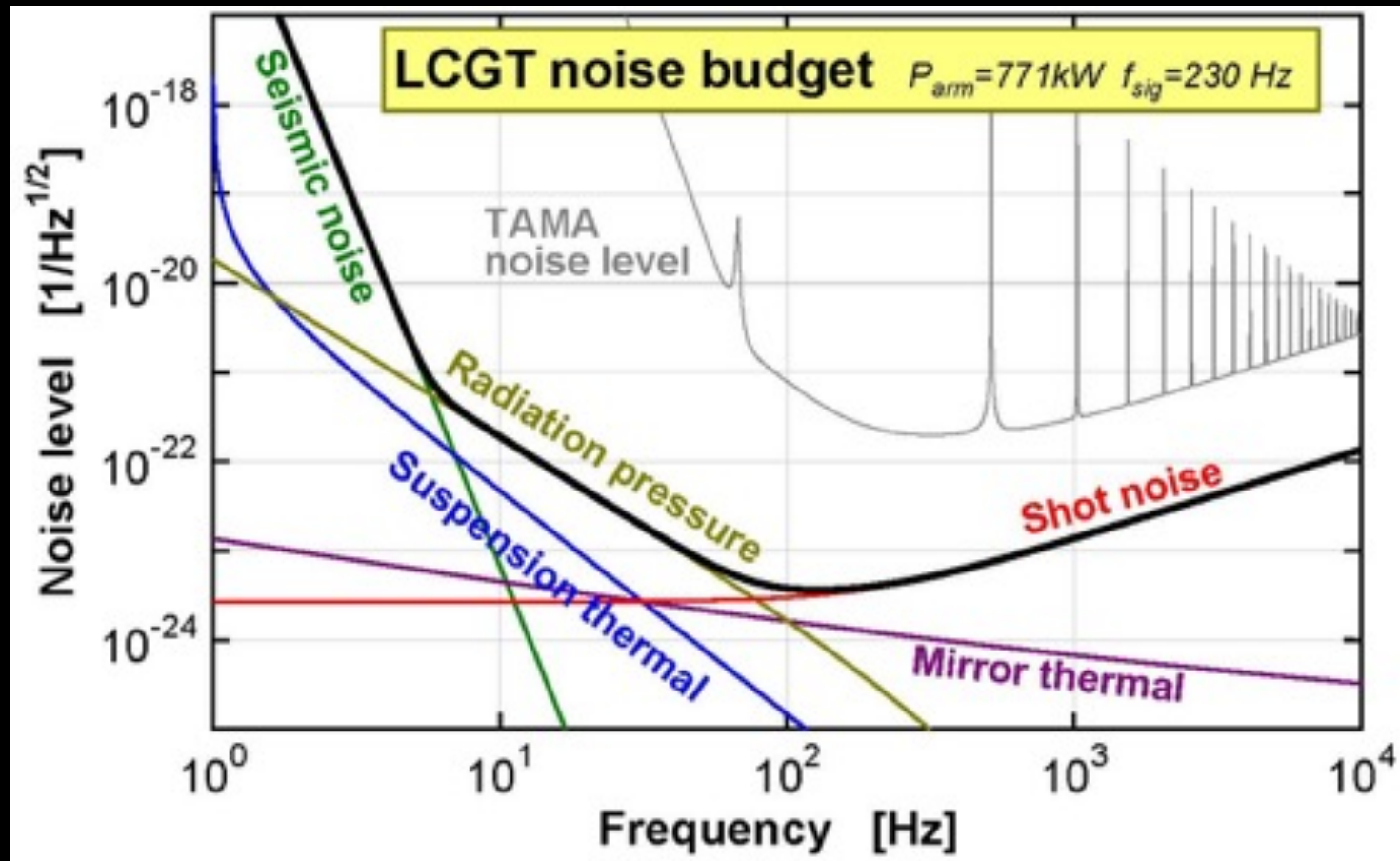


Ligo Hanford (4 km)



Detection: Hz-kHz

- Hz-kHz: ground-based interferometric detectors
Ligo-Virgo-Kagra



LCGT = Kagra

LIGO in 2015

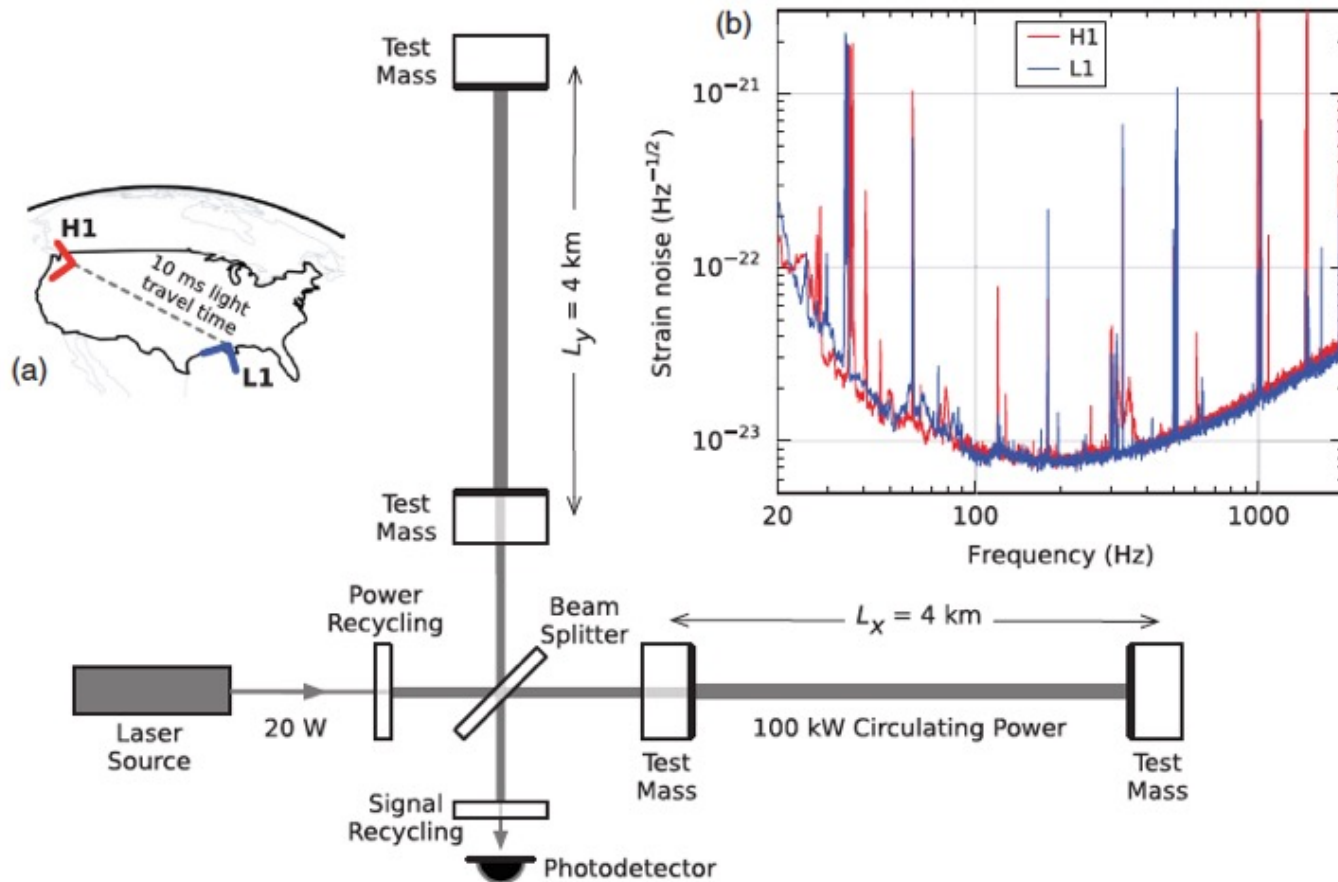
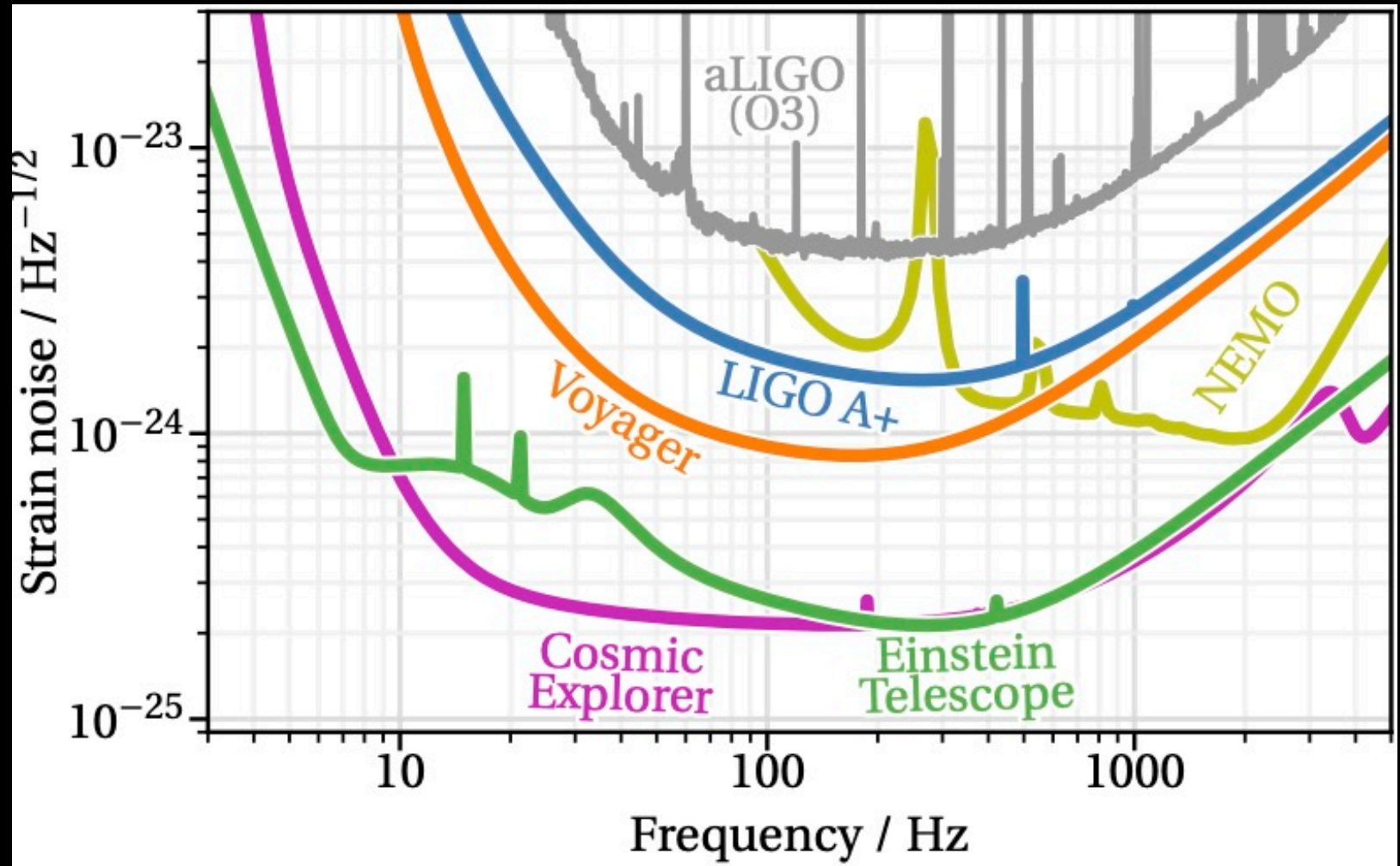


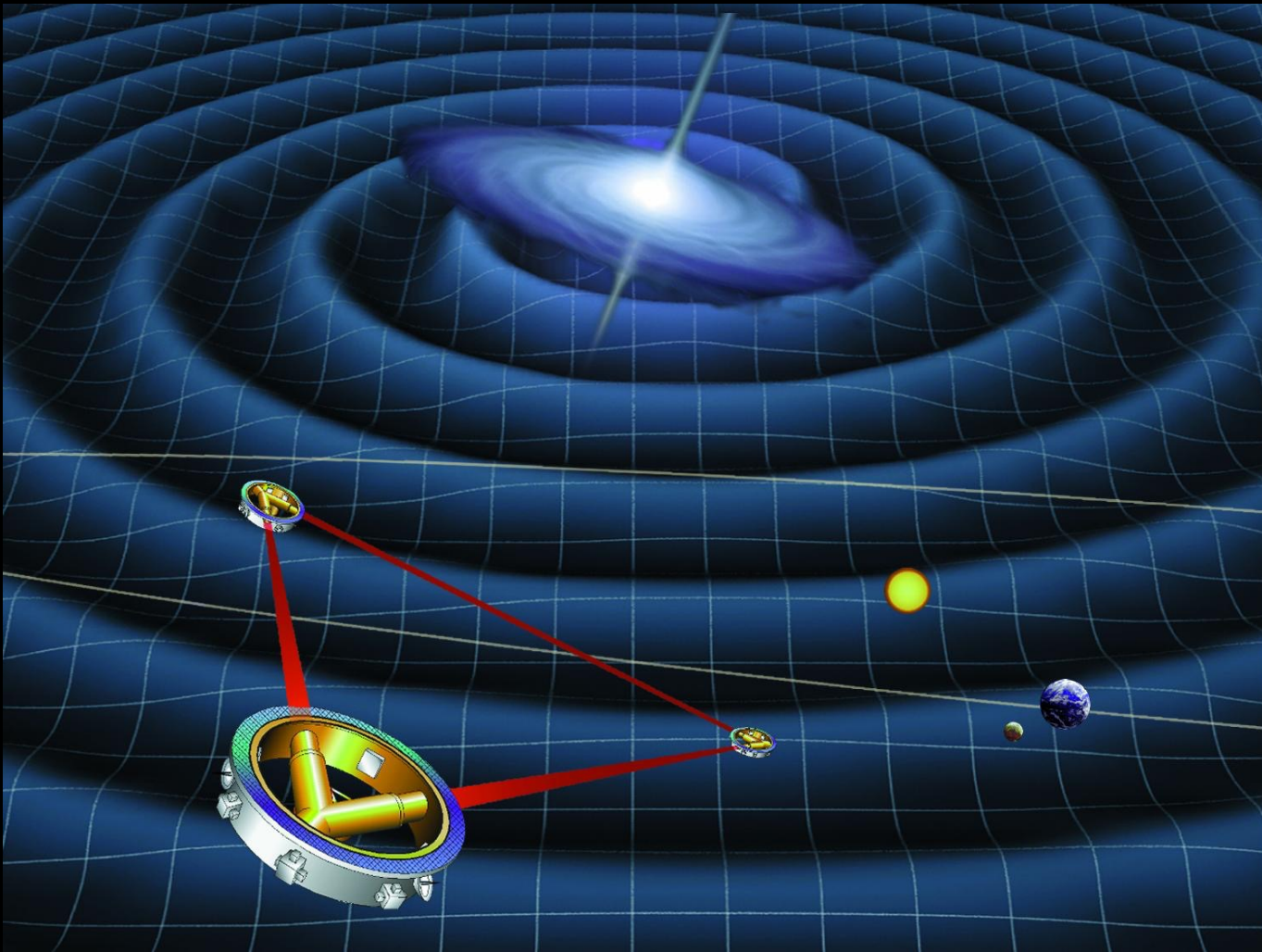
FIG. 3. Simplified diagram of an Advanced LIGO detector (not to scale). A gravitational wave propagating orthogonally to the detector plane and linearly polarized parallel to the 4-km optical cavities will have the effect of lengthening one 4-km arm and shortening the other during one half-cycle of the wave; these length changes are reversed during the other half-cycle. The output photodetector records these differential cavity length variations. While a detector's directional response is maximal for this case, it is still significant for most other angles of incidence or polarizations (gravitational waves propagate freely through the Earth). *Inset (a)*: Location and orientation of the LIGO detectors at Hanford, WA (H1) and Livingston, LA (L1). *Inset (b)*: The instrument noise for each detector near the time of the signal detection; this is an amplitude spectral density, expressed in terms of equivalent gravitational-wave strain amplitude. The sensitivity is limited by photon shot noise at frequencies above 150 Hz, and by a superposition of other noise sources at lower frequencies [47]. Narrow-band features include calibration lines (33–38, 330, and 1080 Hz), vibrational modes of suspension fibers (500 Hz and harmonics), and 60 Hz electric power grid harmonics.

Landscape for ground-based detectors



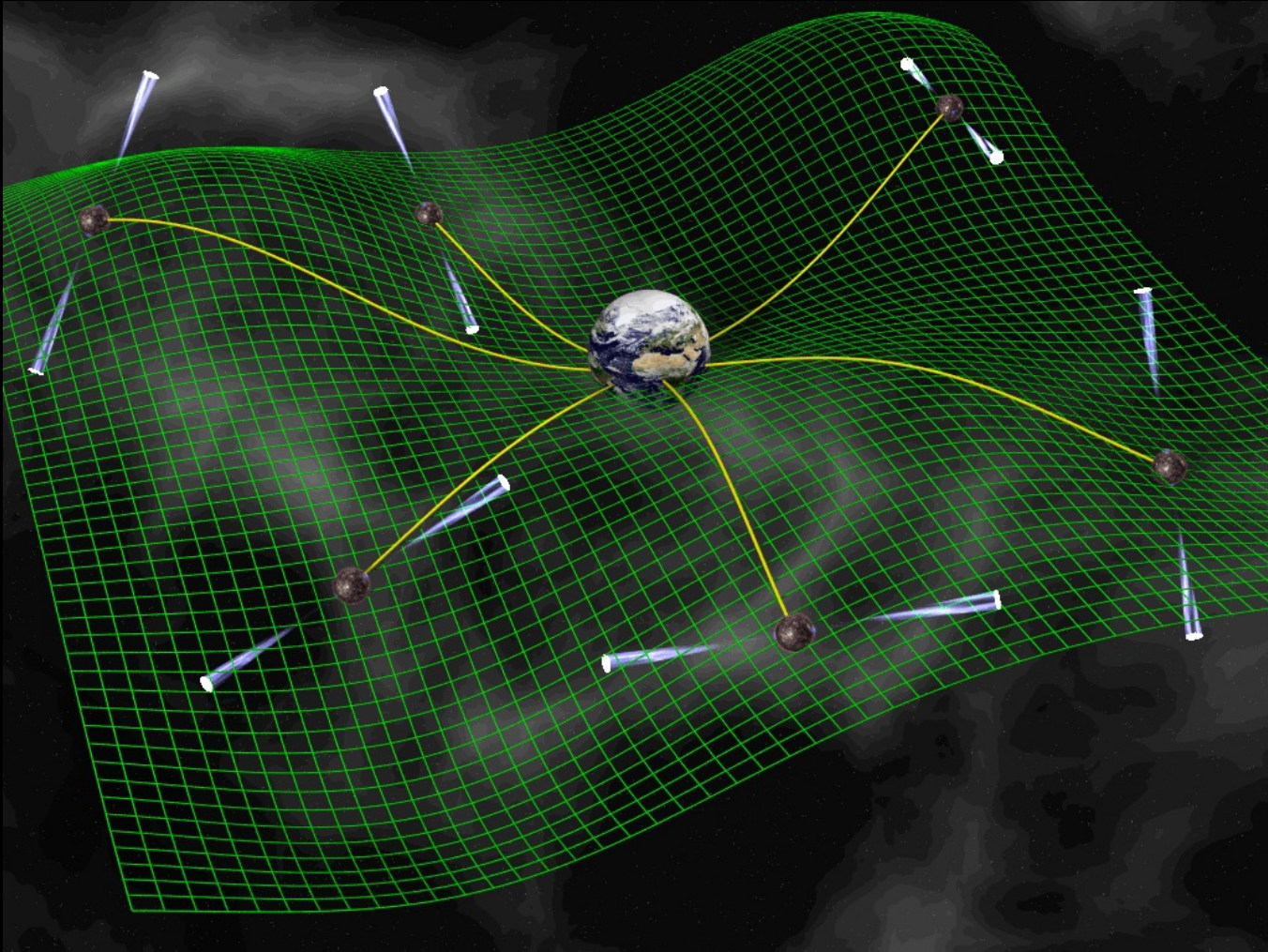
Detection: mHz

- mHz: space-based detectors – arms of $2.5 \cdot 10^6$ km
- LISA: ESA Cosmic Vision, 2032 ?

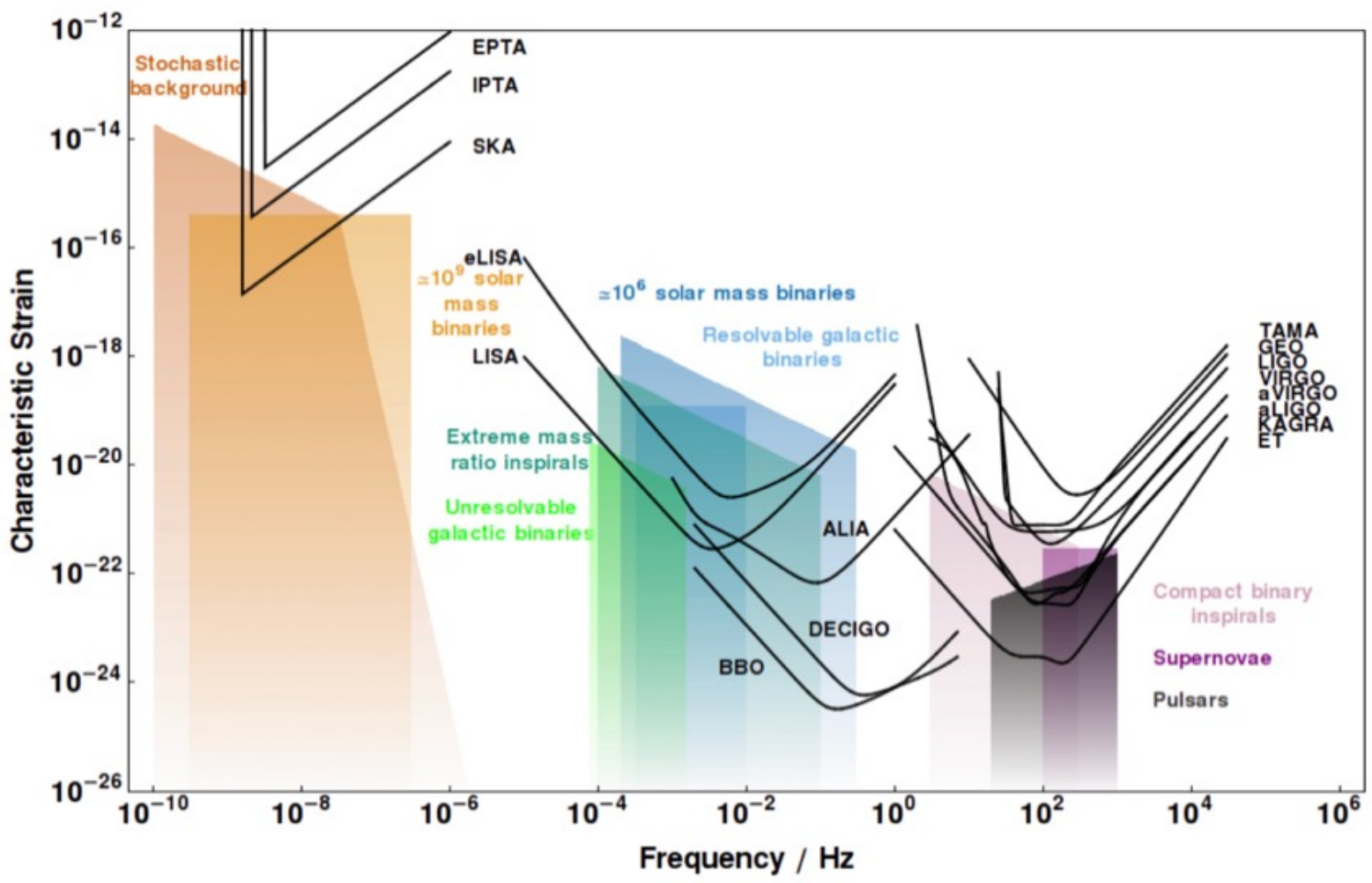


Detection: nHz

- nHz: different method = pulsar timing array (PTA)



Detection technique over ~12 decades



Gravitational Waves: astrophysical sources

Three conditions to be a powerful source of gravitational waves

- GW power: $L_{\text{GW}} = \frac{G}{5c^5} \langle \ddot{Q}_{ij} \ddot{Q}^{ij} \rangle$
- Source: mass M ; size R ; internal velocities v
quadrupole: $Q \sim s M R^2$ (s = dimensionless geom. factor, $s = 0$ at spherical symmetry)

- GW power: $L \sim \frac{c^5}{5G} s^2 \Xi^2 \beta^6$ with $\Xi = \frac{GM}{Rc^2}$
 $\beta = \frac{v}{c}$
- Three conditions must be simultaneously fulfilled to reach a high GW power:

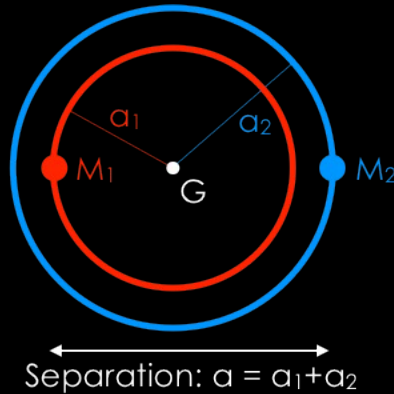
- (1) as far as possible from spherical symmetry (**high s**)
- (2) compact (**high Ξ**)
- (3) internal motion at relativistic speed (**high β**)

Three conditions to be a powerful source of gravitational waves

- GW power: $L \sim \frac{c^5}{5G} s^2 \Xi^2 \beta^6$ with $\Xi = \frac{GM}{Rc^2}$
 $\beta = \frac{v}{c}$
- Three conditions:
 - (1) as far as possible from spherical symmetry (high s)
 - (2) compact (high Ξ)
 - (3) internal motion at relativistic speed (high β)
- Last orbits/merger of a binary system of compact objects (WD, NS, BH): best sources
- Core-collapse of a massive star: (1) only moderately fulfilled, much less powerful sources

Binary system: inspiral phase

- Circular orbit:



$$M = M_1 + M_2$$

$$\mu = \frac{M_1 M_2}{M_1 + M_2}$$

- 3d law of Kepler:

$$\omega = \sqrt{\frac{GM}{a^3}} = \text{orbital frequency}$$

- GW power:

$$L_{\text{GW}} = \frac{32G^4 M^3 \mu^2}{5a^5 c^5}$$

Total energy

- First relativistic correction:

$$\frac{dE}{dt} = -L_{\text{GW}} \quad E = -\frac{GM\mu}{2a}$$

⇒ evolution $a(t)$ and merger time

Binary system: inspiral phase

- Evolution: $a(t) = a_0 \left(1 - \frac{t}{\tau_c} \right)^{1/4}$

- Merger time: $\tau_c = \frac{5}{256} \frac{c^5 a_0^4}{G^3 M^2 \mu}$

BNS 1.5+1.5 M_\odot

with $a_0 = 10^{-3}$ AU: 50 kyr

with $a_0 = 0.02$ AU: 15 Gyr ...

Faster evolution for more massive objects.

Binary system: inspiral phase

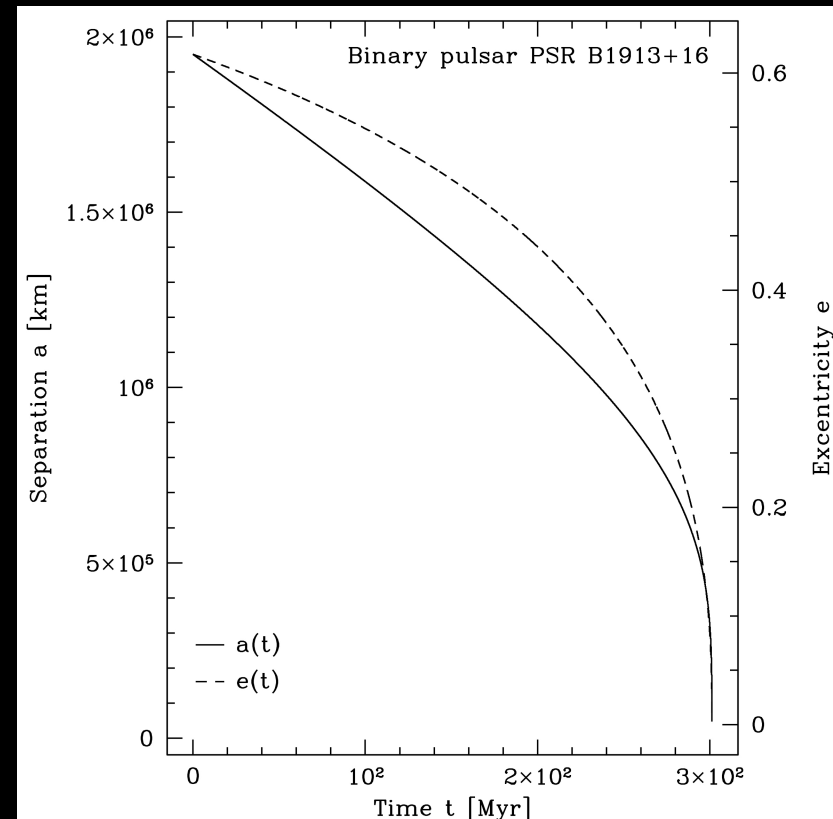
- General case (see e.g. living review in relativity by L. Blanchet)

$$\frac{dE}{dt} = -L_{\text{GW}} \quad \frac{dJ}{dt} = -\dot{J}_{\text{GW}}$$

$$\frac{da}{dt} = -\frac{64}{5} \frac{G^3 M^2 \mu}{c^5 a^3} \frac{1 + \frac{73}{24}e^2 + \frac{37}{96}e^4}{(1 - e^2)^{7/2}},$$
$$\frac{de}{dt} = -\frac{304}{15} \frac{G^3 M^2 \mu e}{c^5 a^4} \frac{1 + \frac{121}{304}e^2}{(1 - e^2)^{5/2}}.$$

- (1) circularization ; (2) merger

PSR B1913+16 will merge
in 320 Myr.



Binary system: inspiral phase

- GW signal at distance D :

$$h_{ij}(t) = -h \begin{pmatrix} \cos\left(2\omega\left(t - \frac{D}{c}\right)\right) & \sin\left(2\omega\left(t - \frac{D}{c}\right)\right) & 0 \\ \sin\left(2\omega\left(t - \frac{D}{c}\right)\right) & -\cos\left(2\omega\left(t - \frac{D}{c}\right)\right) & 0 \\ 0 & 0 & 0 \end{pmatrix}$$

frequency: twice the orbital frequency

amplitude: $h = \frac{4G\mu a^2 \omega^2}{Dc^4}$ for a detector in a plane parallel to the orbital plane

general: modulation $1 + \cos^2(i)$
(degeneracy distance-inclination)

Binary system: inspiral phase

- Evolution: $a(t) = a_0 \left(1 - \frac{t}{\tau_c}\right)^{1/4}$

$$\nu(t) = \frac{2\omega(t)}{2\pi} = \frac{1}{\pi} \underbrace{\sqrt{\frac{GM}{a_0^3}}}_{=\nu_0} \left(1 - \frac{t}{\tau_c}\right)^{-3/8}$$

$$\dot{\nu} \nu^{-11/3} = \frac{96\pi^{8/3}}{5} \left(\frac{GM}{c^3}\right)^{5/3} = \text{cst}$$

- Chirp mass: $\mathcal{M} = M^{2/5} \mu^{3/5}$

Binary system: inspiral phase

Merger time:

$$\begin{aligned}\tau_c &= \frac{5}{256} \frac{c^5 a_0^4}{G^3 M^2 \mu}, \\ &= \frac{5}{32} \frac{a_0^4}{c (2GM/c^2)^2 (2G\mu/c^2)}, \\ &= 5 \times 10^4 \text{ yr} \left(\frac{M}{3 M_\odot} \right)^{-2} \left(\frac{\mu}{0.75 M_\odot} \right)^{-1} \left(\frac{a_0}{10^{-3} \text{ AU}} \right)^4.\end{aligned}$$

Amplitude:

$$\begin{aligned}h(t) &= 4 \frac{G\mu a^2 \omega^2}{c^4} \frac{1}{D} = 4 \left(\frac{G\mu}{ac^2} \right) \left(\frac{GM}{Dc^2} \right) \\ &\simeq 4 \times 10^{-21} \left(\frac{M}{3 M_\odot} \right) \left(\frac{\mu}{0.75 M_\odot} \right) \left(\frac{a}{10^{-6} \text{ AU}} \right)^{-1} \left(\frac{D}{1 \text{ Mpc}} \right)^{-1}, \\ &= 4 \frac{G^{5/3} \mu M^{2/3} \omega^{2/3}}{c^4} \frac{1}{D} = 4 \frac{G^{5/3} M^{5/3} \omega^{2/3}}{c^4} \frac{1}{D} \\ &\simeq 6 \times 10^{-21} \left(\frac{M}{1.3 M_\odot} \right) \left(\frac{\nu}{100 \text{ Hz}} \right)^{2/3} \left(\frac{D}{1 \text{ Mpc}} \right)^{-1}.\end{aligned}$$

Chirp mass:

$$\mathcal{M} = \mu^{3/5} M^{2/5} = \frac{(M_1 M_2)^{3/5}}{M^{1/5}}.$$

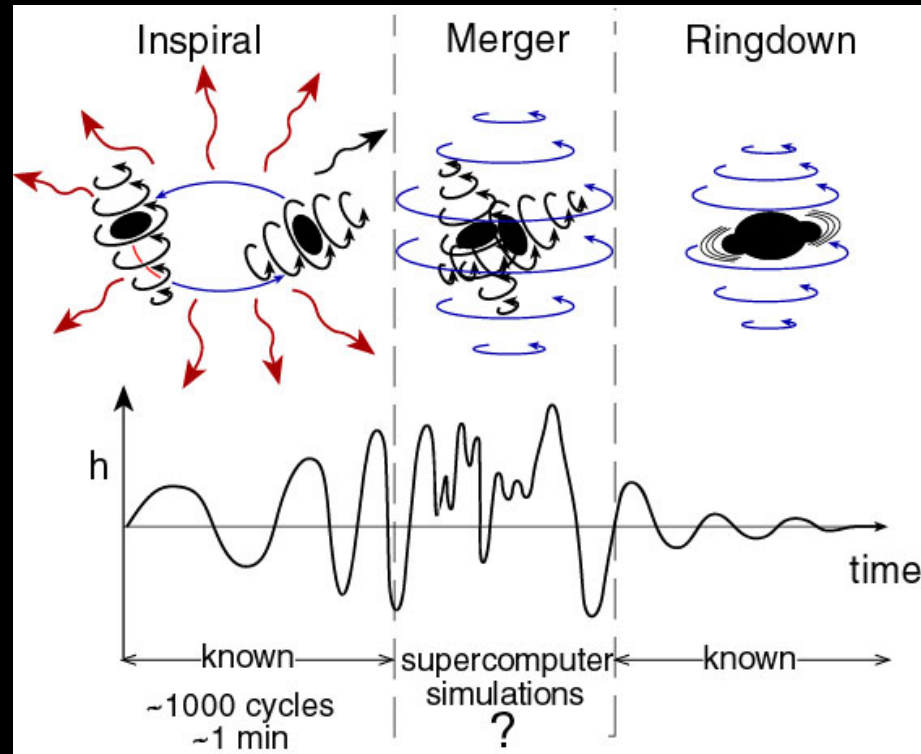
Binary system: inspiral phase

- Inspiral: physical diagnostics
- **Frequency evolution: chirp mass**
- **Amplitude: distance (-inclination)**
- Higher order (PPN, Blanchet et al.):
masses, spins,
tidal effects in last orbits (constraint on EOS), etc.
- **Frequency at merger? For black holes: $a_{\text{merger}} \sim R_{\text{ISCO}}$**

Then $\nu_{\text{merg}} = \frac{1}{\pi} \sqrt{\frac{GM}{a_{\text{merger}}^3}} \propto M^{-1}$

LVK: stellar mass
LISA: SMBH

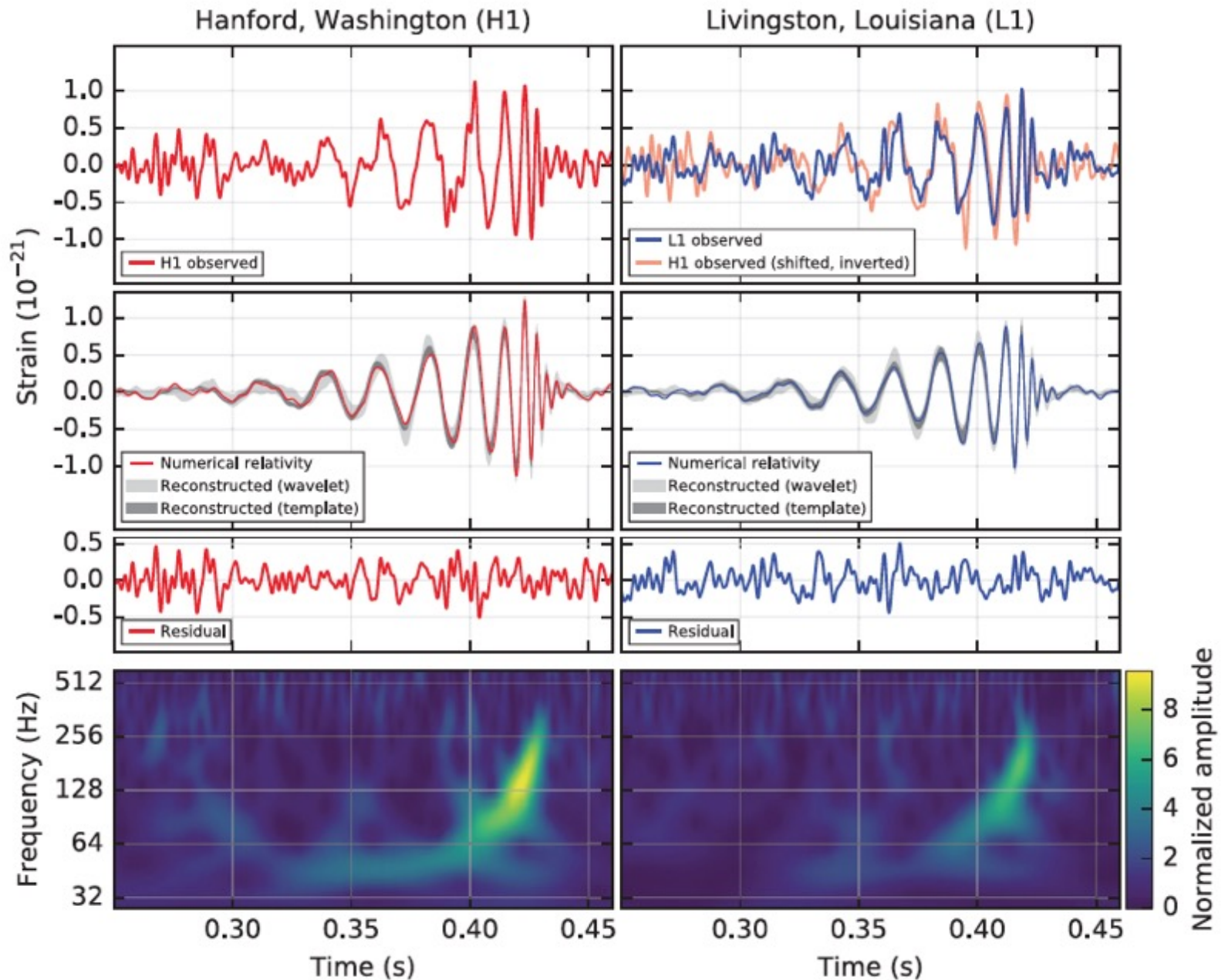
Binary system:



- **Inspiral**: high accuracy prediction (PPN)
= **characterization of the initial system (e.g. M_1, M_2)**
- **Merger**: highly uncertain (numerical relativity)
- **Ringdown**: high accuracy prediction (perturbation theory in Kerr metric) = **characterization of the final BH (M, a)**

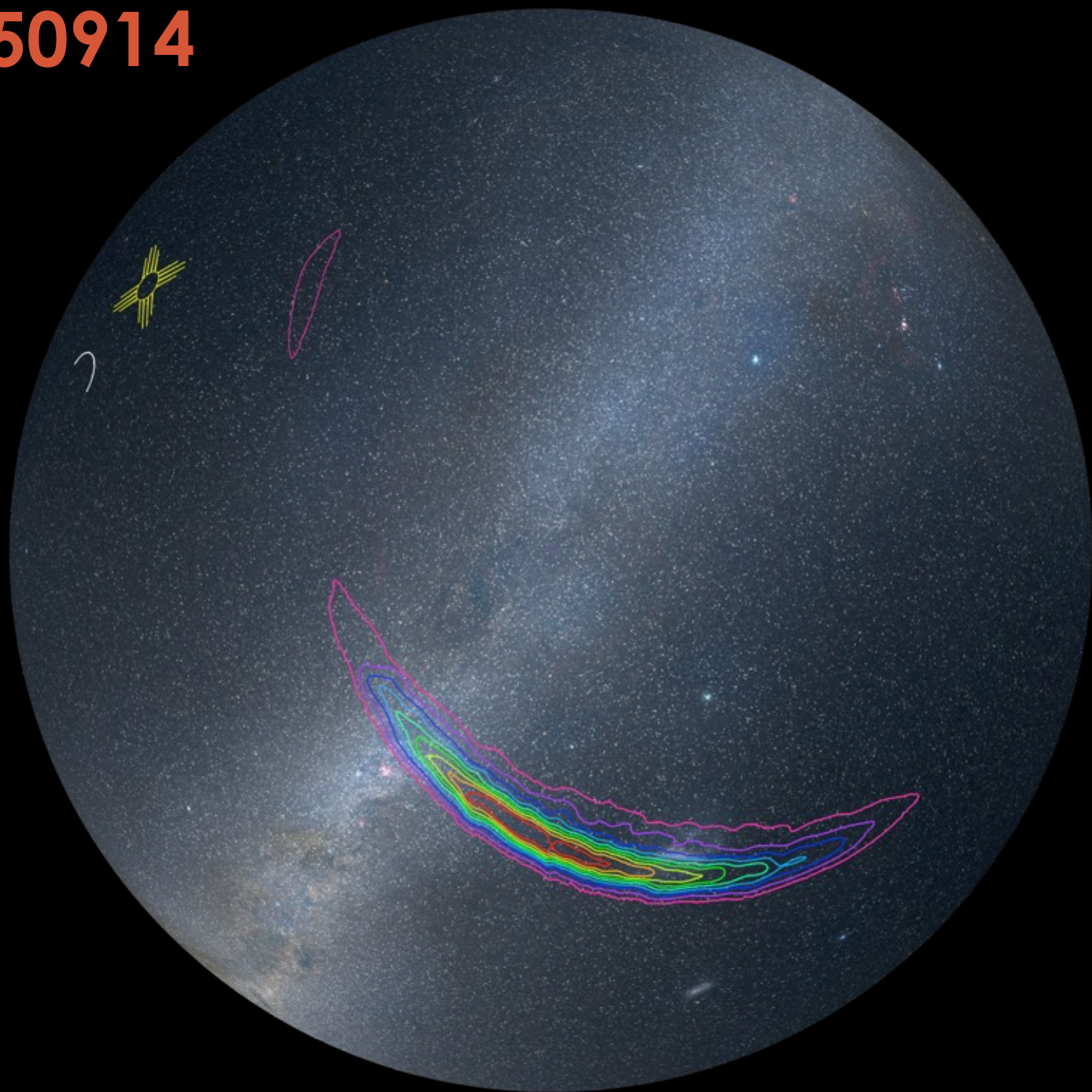
GW150914

Delay ~ 7 ms \rightarrow localization



SNR = 24

GW150914

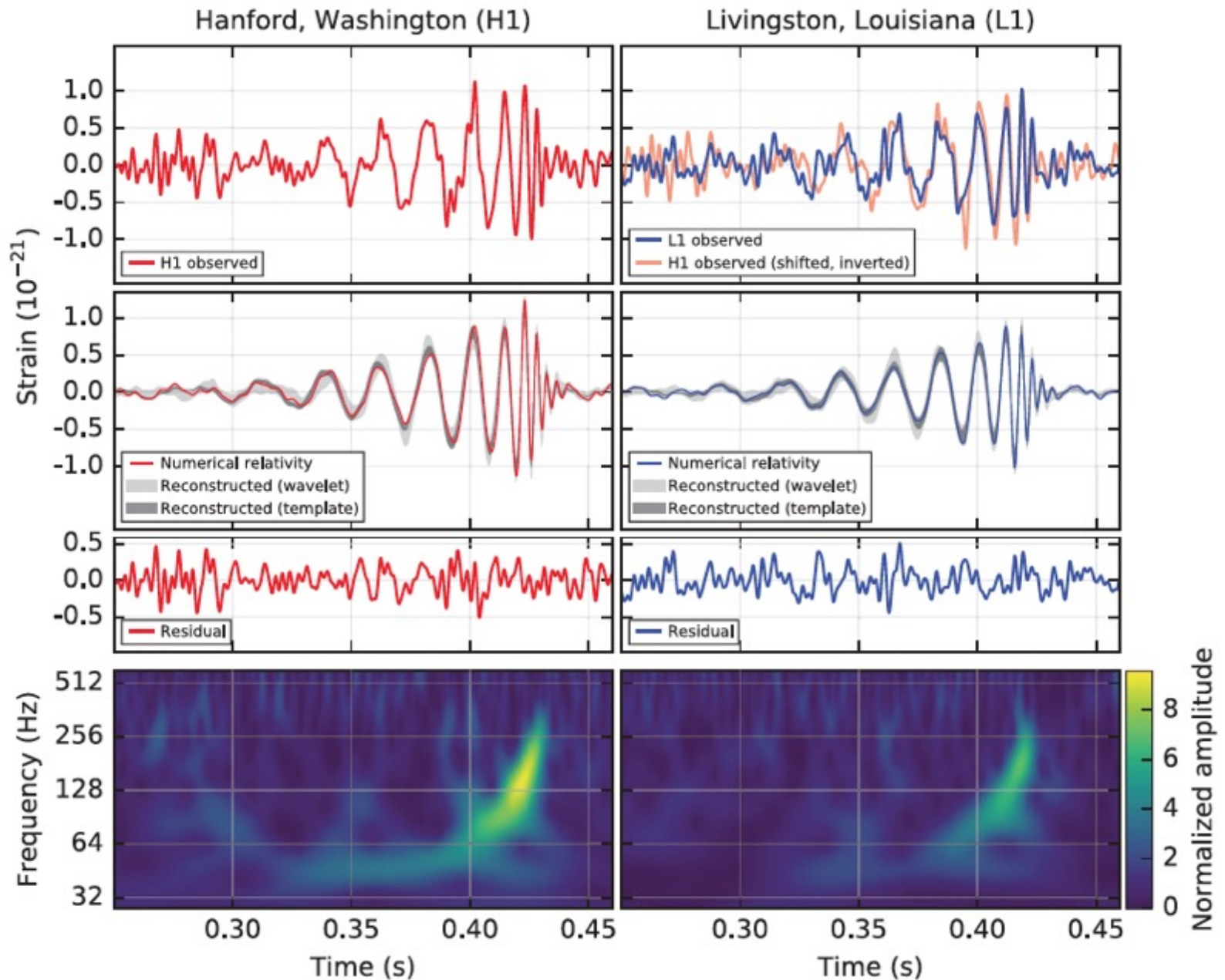


GW150914

Inspiral/
Frequency
evolution:

masses

$$\begin{aligned} \mathcal{M} &= 28 M_{\odot} \\ M_1 &= 36 M_{\odot} \\ M_2 &= 29 M_{\odot} \end{aligned}$$

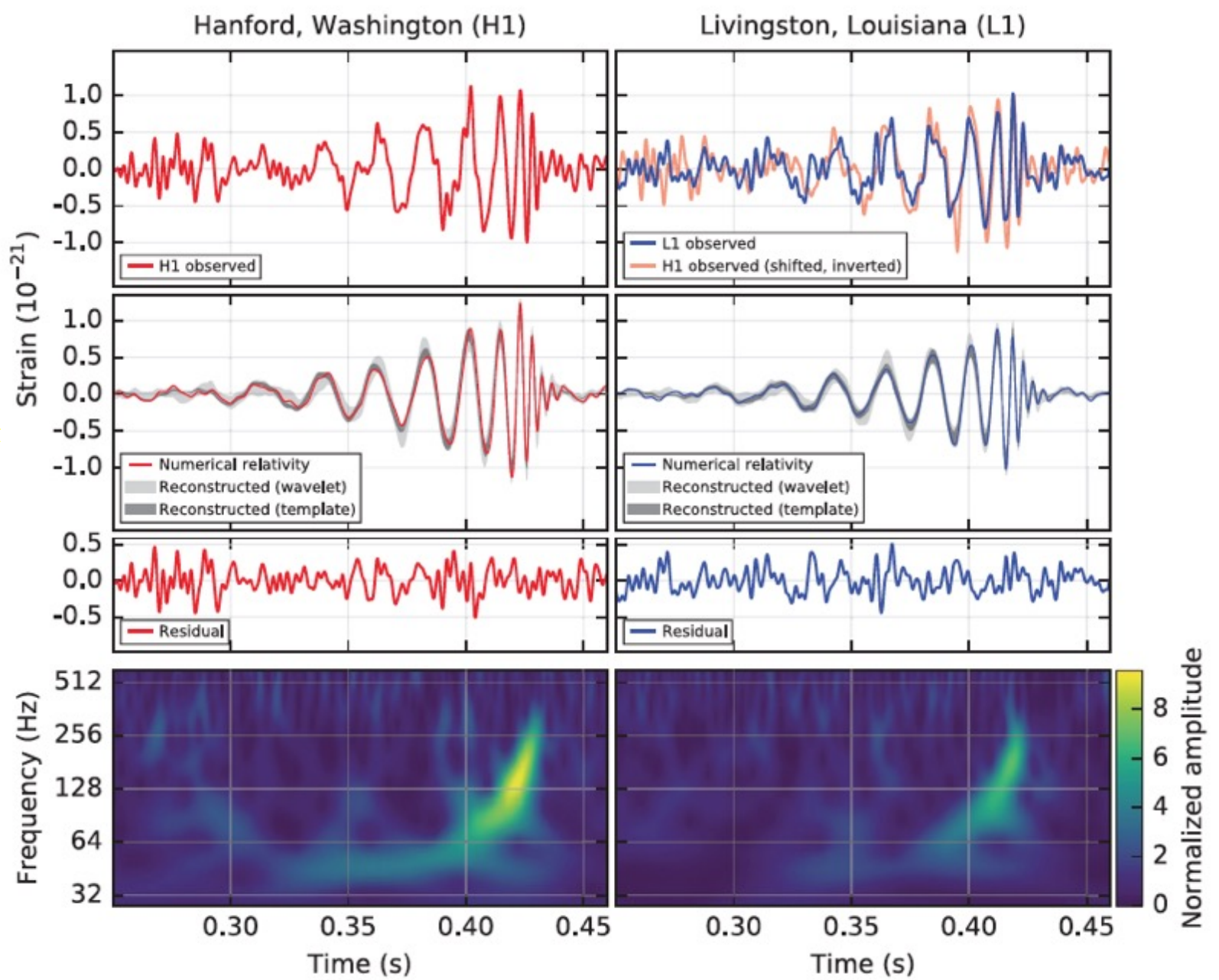


GW150914

Inspiral/
Amplitude
+
chirp mass:

distance
/inclination

D = 410 Mpc



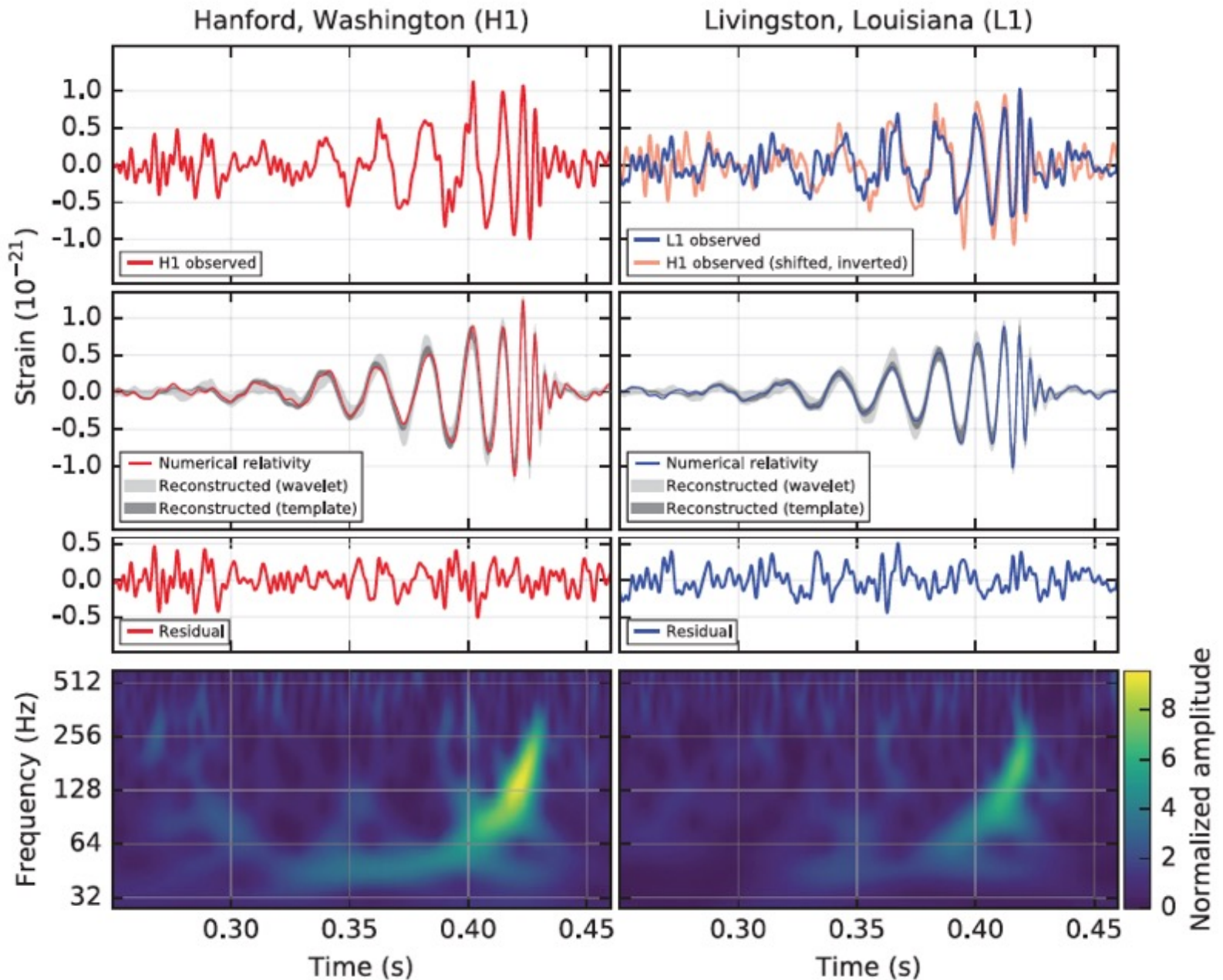
GW150914

Ringdown

final BH

$M = 62 M_{\odot}$

$a = 0.67$



GW150914

Energy emitted as GW:
 $36+29-62 \sim 3 M_{\odot} c^2$!

Efficiency: $3/(36+29)=5\%$
in agreement with Numerical GR

TABLE I. Source parameters for GW150914. We report median values with 90% credible intervals that include statistical errors, and systematic errors from averaging the results of different waveform models. Masses are given in the source frame; to convert to the detector frame multiply by $(1+z)$ [90]. The source redshift assumes standard cosmology [91].

Primary black hole mass	$36_{-4}^{+5} M_{\odot}$
Secondary black hole mass	$29_{-4}^{+4} M_{\odot}$
Final black hole mass	$62_{-4}^{+4} M_{\odot}$
Final black hole spin	$0.67_{-0.07}^{+0.05}$
Luminosity distance	410_{-180}^{+160} Mpc
Source redshift z	$0.09_{-0.04}^{+0.03}$

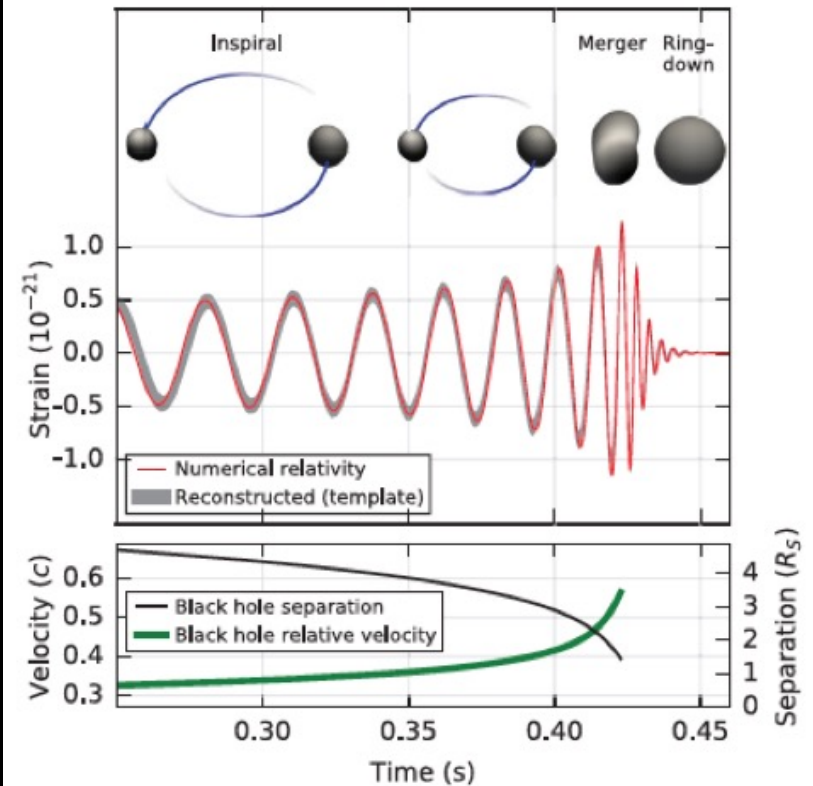


FIG. 2. *Top*: Estimated gravitational-wave strain amplitude from GW150914 projected onto H1. This shows the full bandwidth of the waveforms, without the filtering used for Fig. 1. The inset images show numerical relativity models of the black hole horizons as the black holes coalesce. *Bottom*: The Keplerian effective black hole separation in units of Schwarzschild radii ($R_S = 2GM/c^2$) and the effective relative velocity given by the post-Newtonian parameter $v/c = (GM\pi f/c^3)^{1/3}$, where f is the gravitational-wave frequency calculated with numerical relativity and M is the total mass (value from Table I).

GW150914

Peak GW luminosity:
 $9 \times 10^{22} L_{\odot}$!

~100 the luminosity of all galaxies
in the observable Universe...

TABLE I. Source parameters for GW150914. We report median values with 90% credible intervals that include statistical errors, and systematic errors from averaging the results of different waveform models. Masses are given in the source frame; to convert to the detector frame multiply by $(1+z)$ [90]. The source redshift assumes standard cosmology [91].

Primary black hole mass	$36_{-4}^{+5} M_{\odot}$
Secondary black hole mass	$29_{-4}^{+4} M_{\odot}$
Final black hole mass	$62_{-4}^{+4} M_{\odot}$
Final black hole spin	$0.67_{-0.07}^{+0.05}$
Luminosity distance	410_{-180}^{+160} Mpc
Source redshift z	$0.09_{-0.04}^{+0.03}$

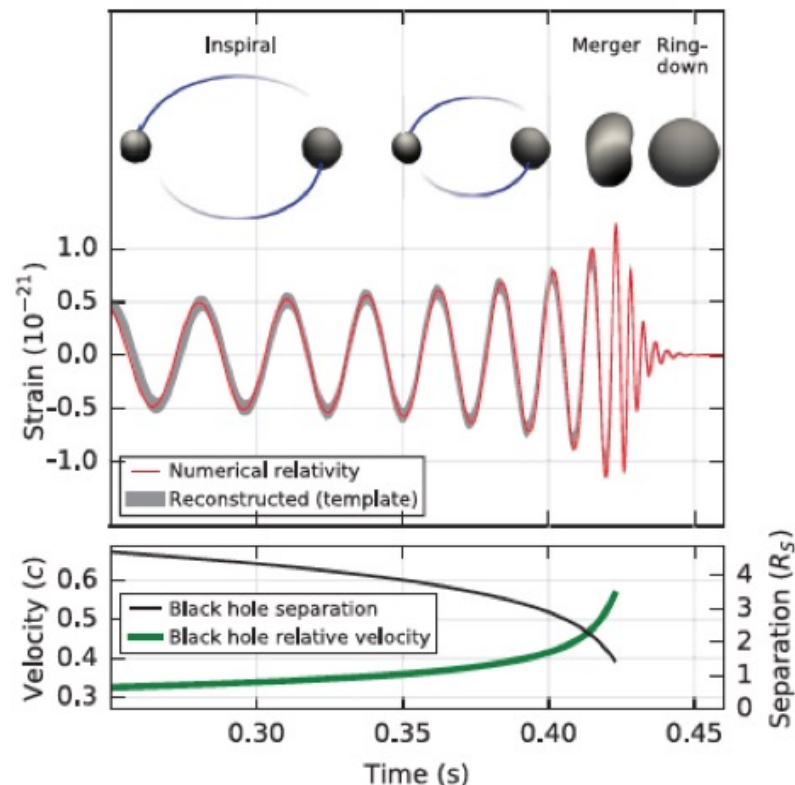


FIG. 2. *Top*: Estimated gravitational-wave strain amplitude from GW150914 projected onto H1. This shows the full bandwidth of the waveforms, without the filtering used for Fig. 1. The inset images show numerical relativity models of the black hole horizons as the black holes coalesce. *Bottom*: The Keplerian effective black hole separation in units of Schwarzschild radii ($R_S = 2GM/c^2$) and the effective relative velocity given by the post-Newtonian parameter $v/c = (GM\pi f/c^3)^{1/3}$, where f is the gravitational-wave frequency calculated with numerical relativity and M is the total mass (value from Table I).

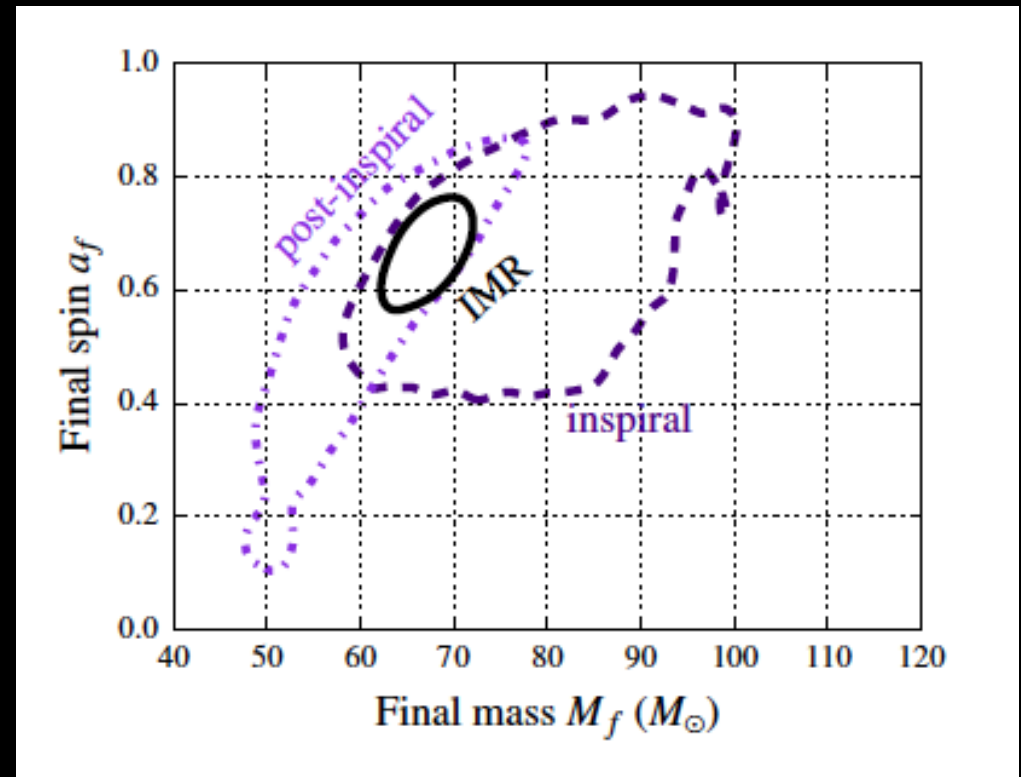
GW150914

- Many more results
- **Several tests of GR**

Inspiral: prediction using only the data in the inspiral phase

Post-inspiral: measure using only the ringdown signal

IMR: measure using all data



- **Limit on graviton mass (delay between the two interferometers): 10^{-22} eV/ c^2 !**

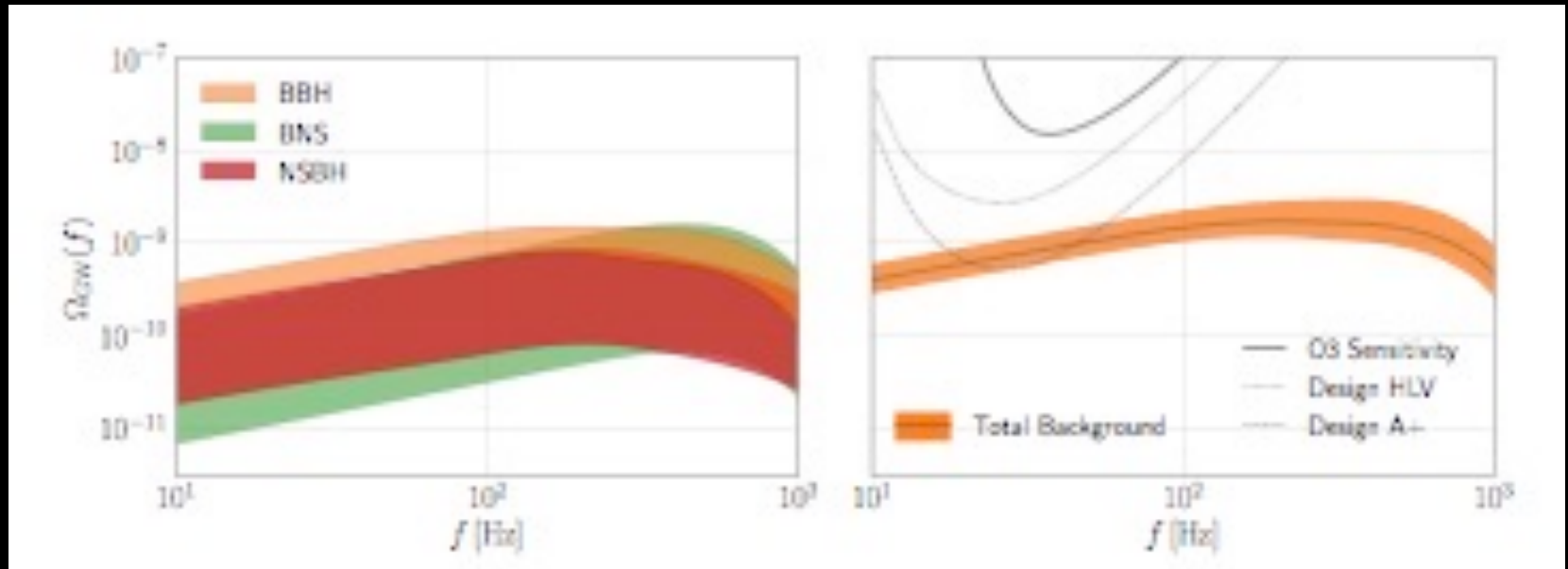
**Gravitational Waves:
backgrounds
(astrophysical / primordial)**

GW background

- See recent review: [Renzini et al. 2022](#)
- **Primordial background** (inflation, ...)
- **Astrophysical background: unresolved sources (detector dependent)** = dominated by mergers
- Stochastic by generation processes (primordial) or due to the large number of unresolved sources (astrophysical).

Perspectives on GWB

- **Best chances of direct detection: astrophysical GWB**
 - SMBH mergers by PTA:
hint with Nanograv 12.5 yr dataset? (Arzoumanian et al. 2020)
 - Stellar mass mergers (BBH, BNS):
LVK at design sensitivity?

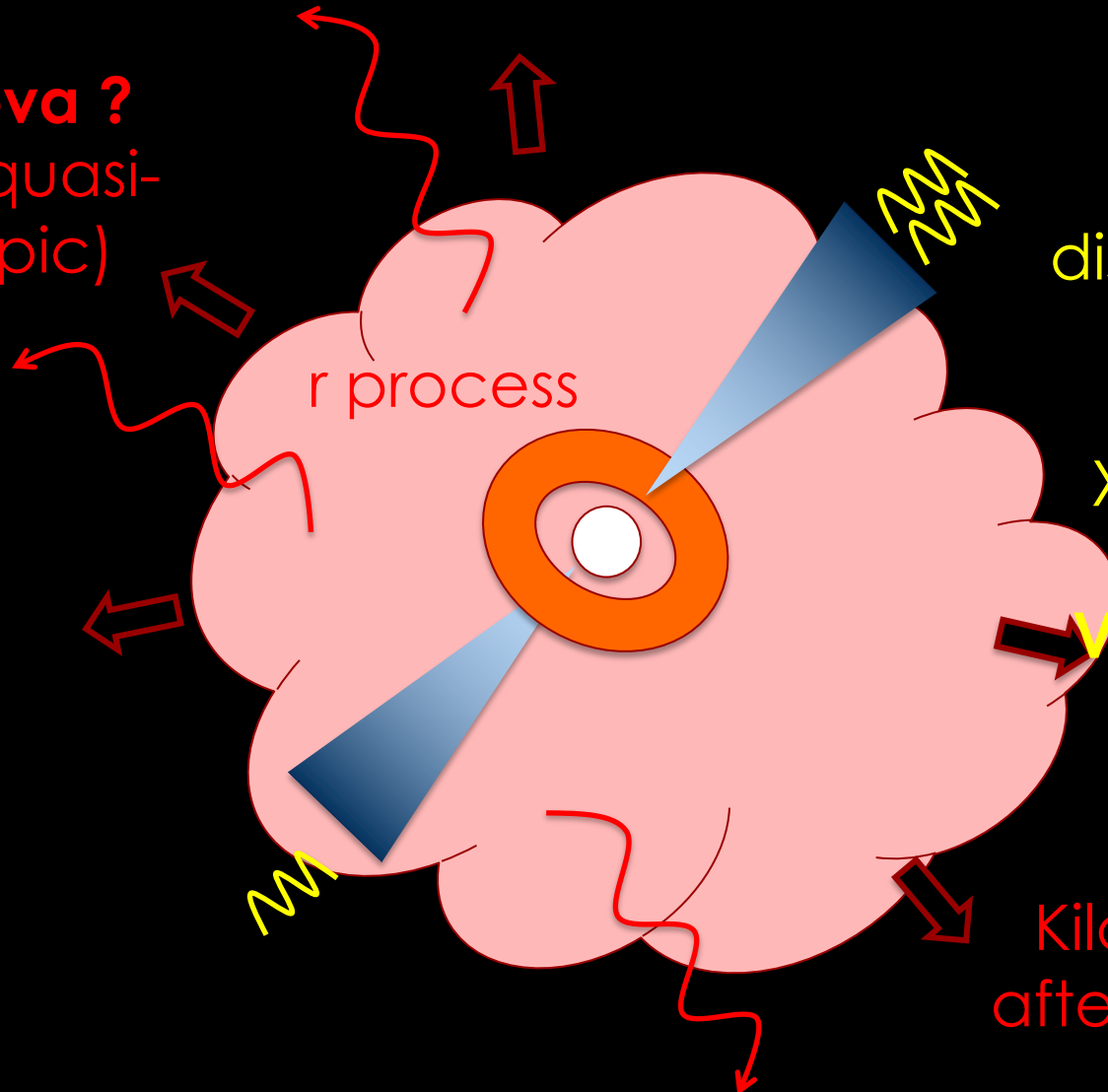


**Multi-messenger astrophysics
with gravitational waves:
the 170817 event**

BNS merger: expected em counterparts

- Pre-2017 predictions

Kilonova ?
(V, IR, quasi-isotropic)



r process

Relativistic jet:

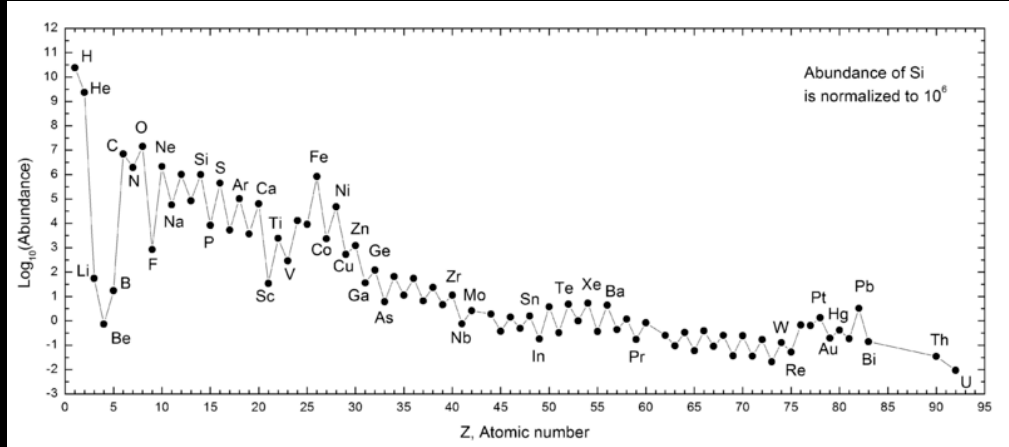
-Short GRB
(internal dissipation: γ -rays)

-Afterglow
(deceleration: X-rays \rightarrow radio)

Very anisotropic
(relativistic beaming)

Kilonova
afterglow ?

Rapide neutron captures



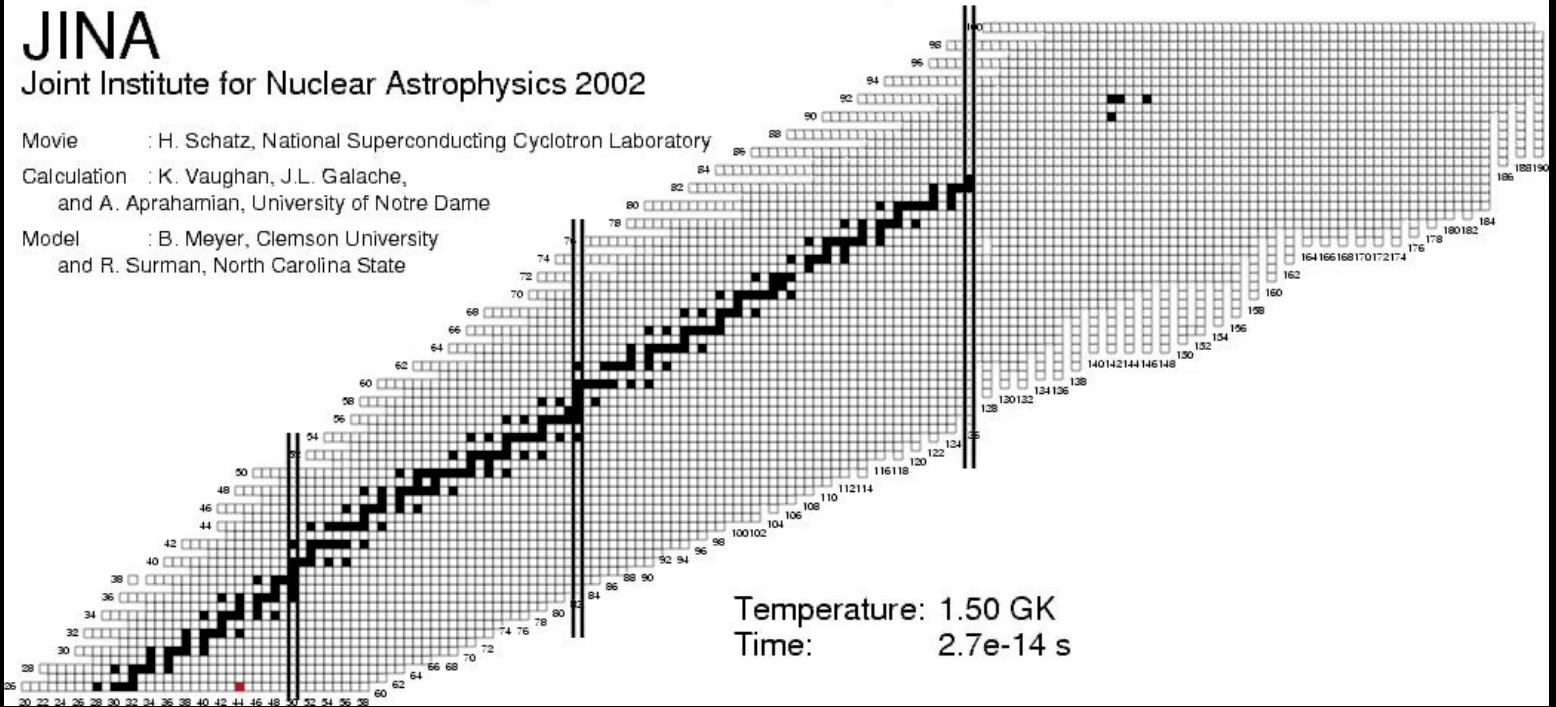
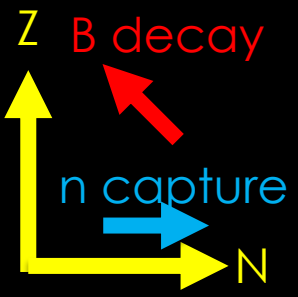
Lodders (2003)

Nucleosynthesis in the r-process

JINA

Joint Institute for Nuclear Astrophysics 2002

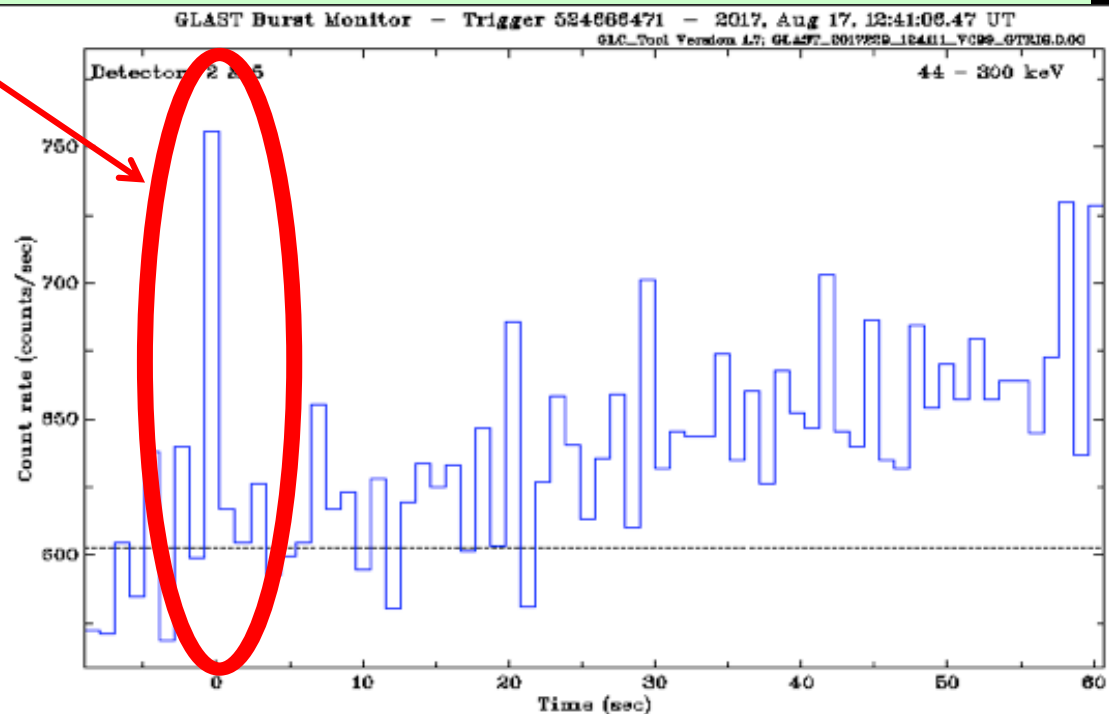
Movie : H. Schatz, National Superconducting Cyclotron Laboratory
 Calculation : K. Vaughan, J.L. Galache, and A. Aprahamian, University of Notre Dame
 Model : B. Meyer, Clemson University and R. Surman, North Carolina State



17 August 2017 - 12:41 TU

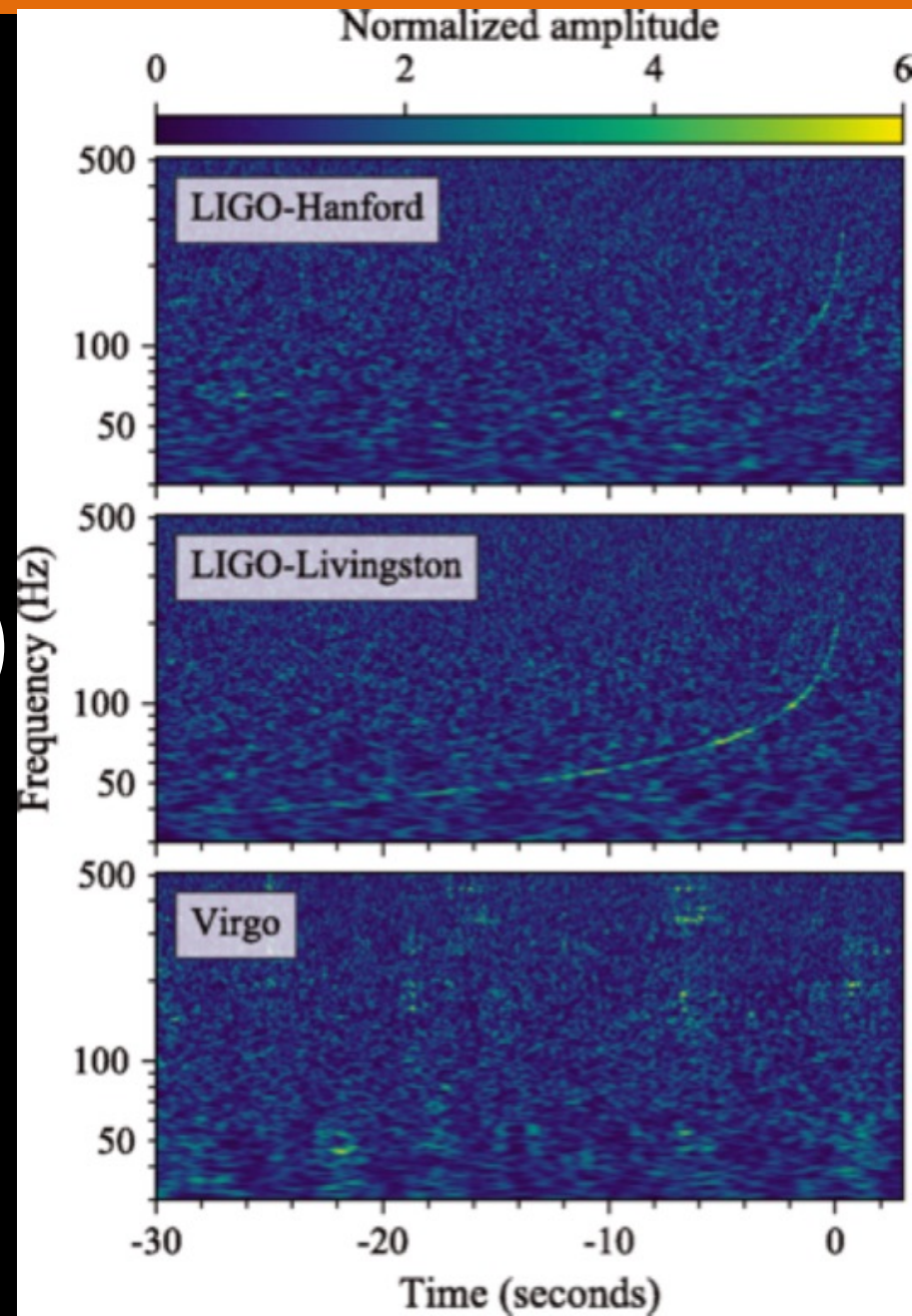
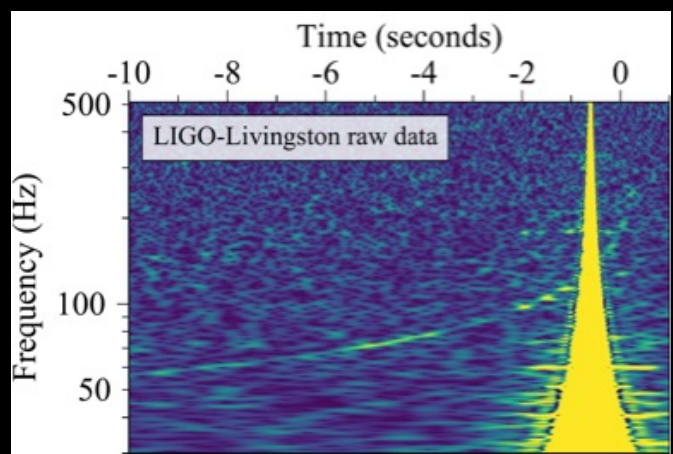
- Detection of GRB 170817A by Fermi/GBM (weak, short)

```
////////////////////////////////////  
TITLE:          GCN/FERMI NOTICE NOTICE_DATE:      Thu 17 Aug 17 12:41:20 UT  
NOTICE_TYPE:    Fermi-GBM Alert RECORD_NUM:          1  
TRIGGER_NUM:    524666471  
GRB_DATE:       17982 MJD:      229 DOY;    17/08/17  
GRB_TIME:       45666.47 SOD {12:41:06.47} UT  
TRIGGER_SIGNIF: 4.8 [sigma]  
TRIGGER_DUR:    0.256 [sec]  
E_RANGE:        3-4 [chan] 47-291 [keV]  
...  
COMMENTS:       Fermi-GBM Trigger Alert  
COMMENTS:       This trigger occurred at  
The LC_URL file will not be created until  
////////////////////////////////////
```



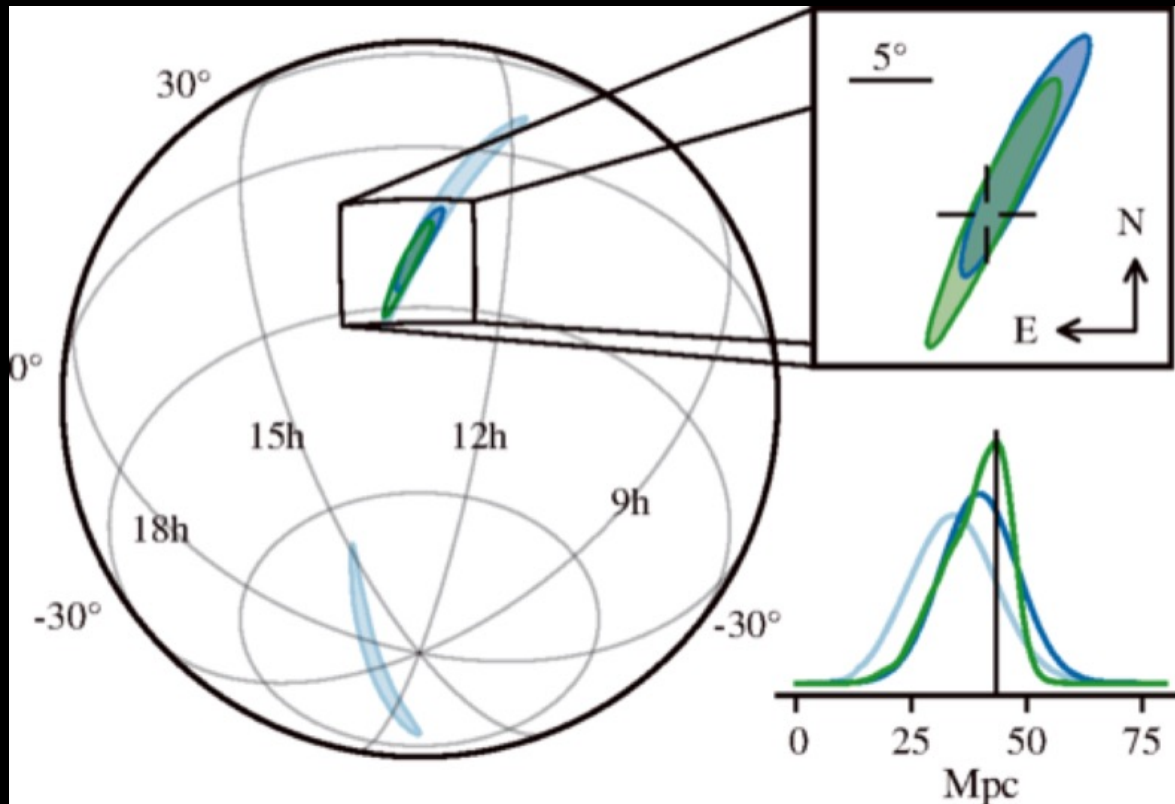
17 August 2017 - 12:47 TU

- Ligo-Virgo: a new merger has been detected 6 min ago, i.e. ~ 2 s before GRB170817A (time coincidence)
 - **First BNS (signal much longer)**
 - **Alert to the community at 13:21** (i.e. 40 min post-merger)
- [delicate analysis: glitch in L1]



Localization of GW170817

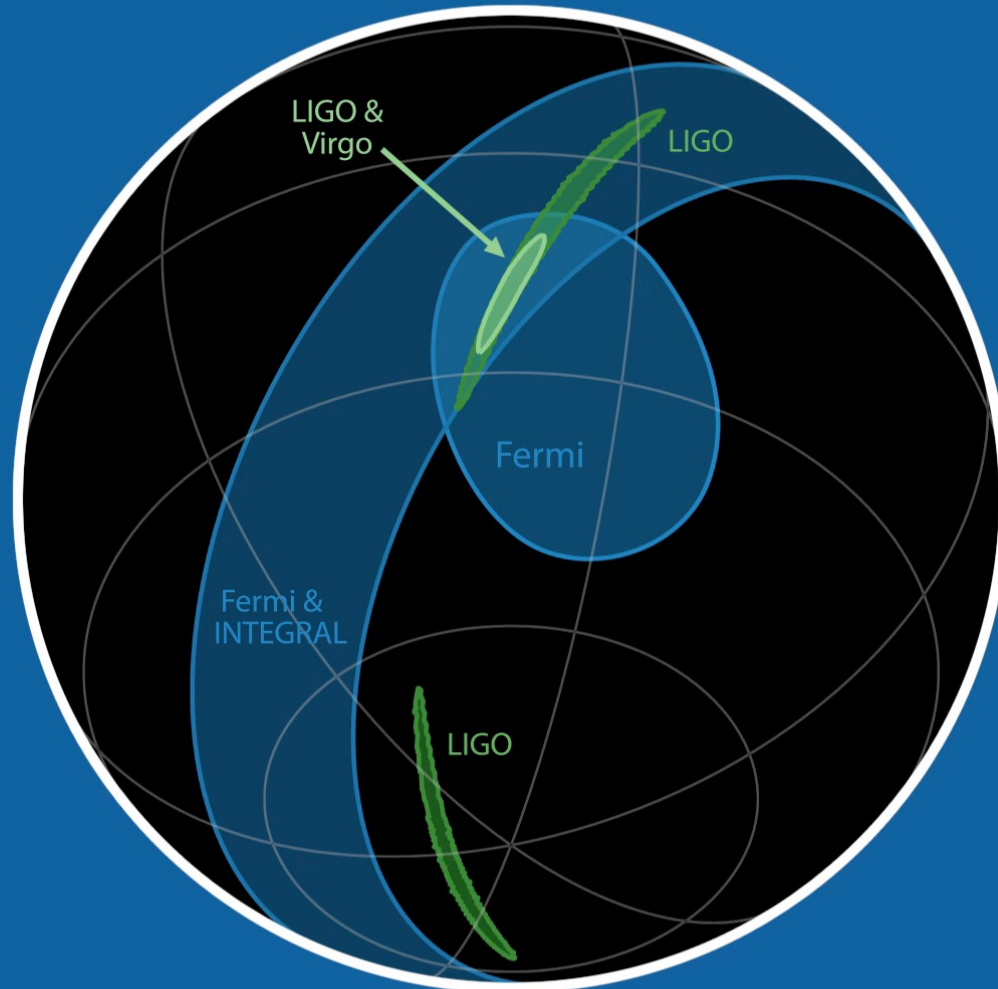
- Detected by LIGO (L+H): 190 deg^2 / distance 40 Mpc
- Detectable by Virgo at 40 Mpc in some directions: reduces the error-box to 30 deg^2 !
- 3D localization sent to the community at 17:54, i.e. 5h post-merger



Galaxy catalogs:
~50 galaxies
In this 3D errorbox.

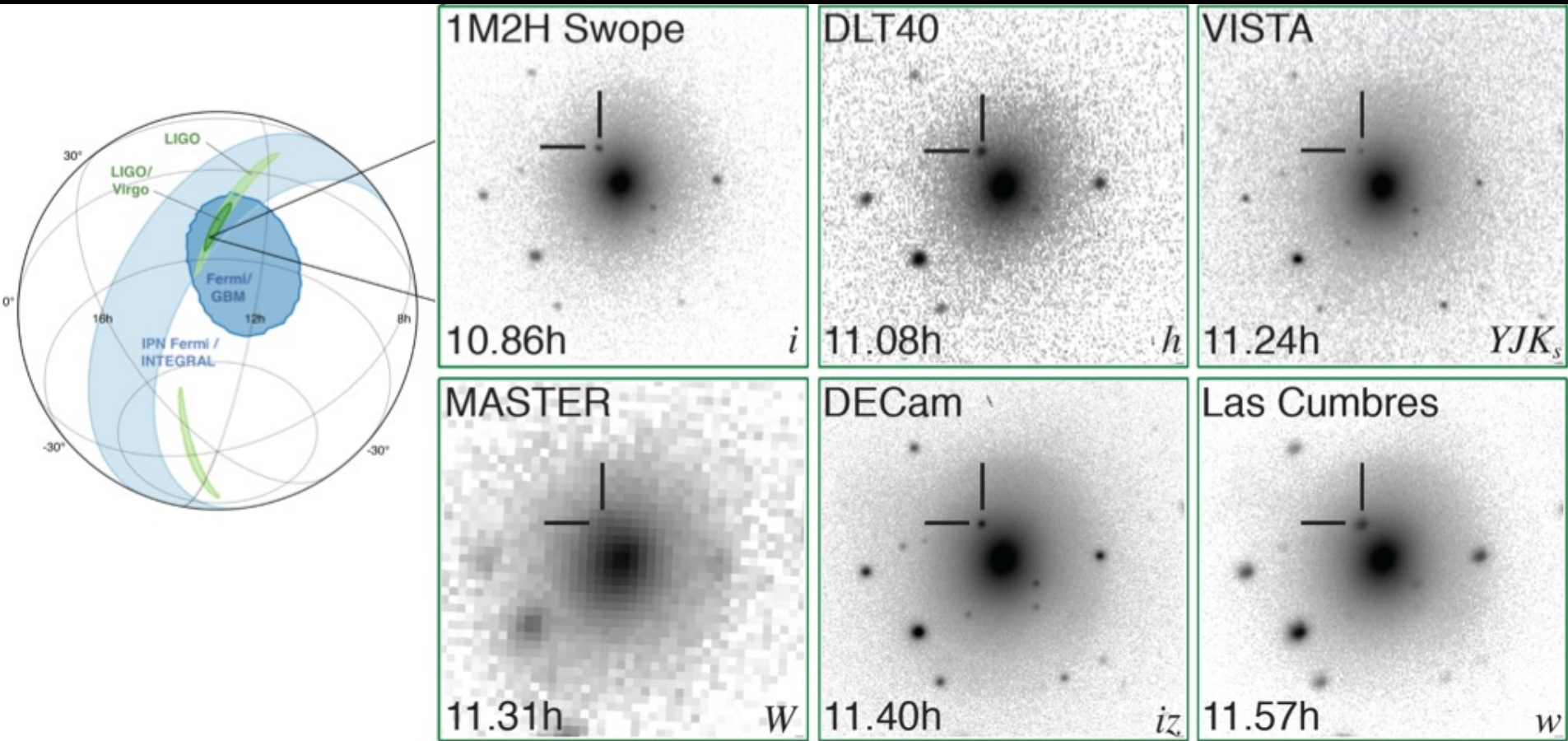
Searching for an em counterpart

- The search starts ~10 hours after the merger (night in Chile)



A kilonova: AT 2017gfo in NGC 4993

- Detection by Swope + 5 other groups at \sim merger+11h



A kilonova: AT 2017gfo in NGC 4993

- AT2017gfo: a unique spectro-photometric follow-up following the detection

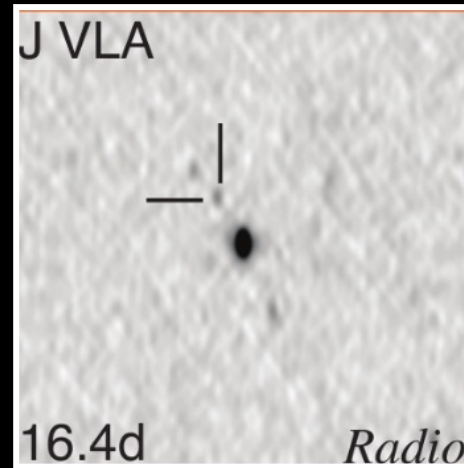
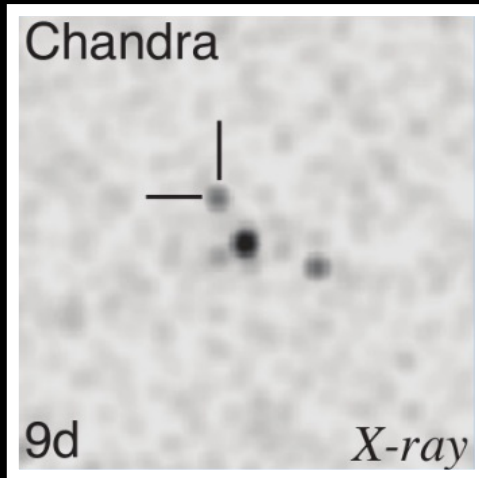
SSS17a



- Accurate localization: search for counterparts at other λ

Counterparts at all wavelengths

- X-rays: detected at merger+9 days (Chandra)
- Radio: detected at merger+16.4 days (VLA)



- This multi-wavelength afterglow peaks after 100 days and was still detectable four years later.

Diagnostic (1) GW

- Inspiral phase detected for more than 100 s
- Post-merger signal not detected

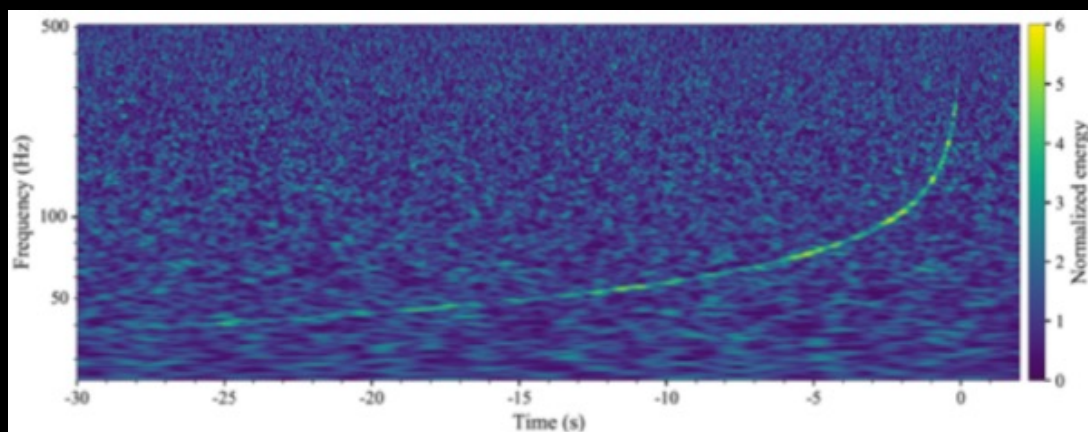


TABLE I. Source properties for GW170817: we give ranges encompassing the 90% credible intervals for different assumptions of the waveform model to bound systematic uncertainty. The mass values are quoted in the frame of the source, accounting for uncertainty in the source redshift.

	Low-spin priors ($ \chi \leq 0.05$)	High-spin priors ($ \chi \leq 0.89$)
Primary mass m_1	1.36–1.60 M_\odot	1.36–2.26 M_\odot
Secondary mass m_2	1.17–1.36 M_\odot	0.86–1.36 M_\odot
Chirp mass \mathcal{M}	$1.188^{+0.004}_{-0.002} M_\odot$	$1.188^{+0.004}_{-0.002} M_\odot$
Mass ratio m_2/m_1	0.7–1.0	0.4–1.0
Total mass m_{tot}	$2.74^{+0.04}_{-0.01} M_\odot$	$2.82^{+0.47}_{-0.09} M_\odot$
Radiated energy E_{rad}	$> 0.025 M_\odot c^2$	$> 0.025 M_\odot c^2$
Luminosity distance D_L	40^{+8}_{-14} Mpc	40^{+8}_{-14} Mpc
Viewing angle Θ	$\leq 55^\circ$	$\leq 56^\circ$
Using NGC 4993 location	$\leq 28^\circ$	$\leq 28^\circ$
Combined dimensionless tidal deformability $\tilde{\Lambda}$	≤ 800	≤ 700
Dimensionless tidal deformability $\Lambda(1.4M_\odot)$	≤ 800	≤ 1400

Diagnostic (1) GW

- Inspiral phase detected for more than 100 s
- Post-merger signal not detected (nature of the remnant?)

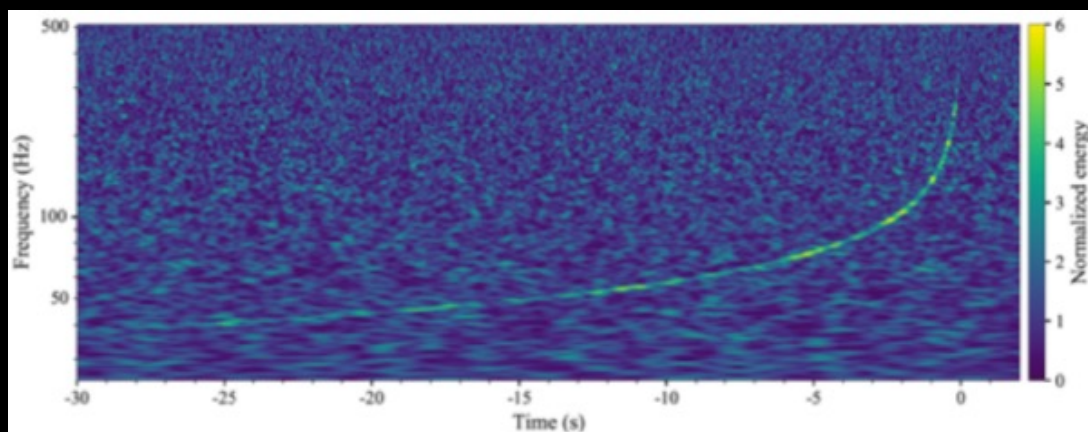


TABLE I. Source properties for GW170817: we give ranges encompassing the 90% credible intervals for different assumptions of the waveform model to bound systematic uncertainty. The mass values are quoted in the frame of the source, accounting for uncertainty in the source redshift.

	Low-spin priors ($ \chi \leq 0.05$)	High-spin priors ($ \chi \leq 0.89$)
Primary mass m_1	1.36–1.60 M_\odot	1.36–2.26 M_\odot
Secondary mass m_2	1.17–1.36 M_\odot	0.86–1.36 M_\odot
Chirp mass \mathcal{M}	1.188 $^{+0.004}_{-0.002}$ M_\odot	1.188 $^{+0.004}_{-0.002}$ M_\odot
Mass ratio m_2/m_1	0.7–1.0	0.4–1.0
Total mass m_{tot}	2.74 $^{+0.04}_{-0.01}$ M_\odot	2.82 $^{+0.47}_{-0.09}$ M_\odot
Radiated energy E_{rad}	$> 0.025 M_\odot c^2$	$> 0.025 M_\odot c^2$
Luminosity distance D_L	40 $^{+8}_{-14}$ Mpc	40 $^{+8}_{-14}$ Mpc
Viewing angle Θ	$\leq 55^\circ$	$\leq 56^\circ$
Using NGC 4993 location	$\leq 28^\circ$	$\leq 28^\circ$
Combined dimensionless tidal deformability $\tilde{\Lambda}$	≤ 800	≤ 700
Dimensionless tidal deformability $\Lambda(1.4M_\odot)$	≤ 800	≤ 1400

BNS: masses

Distance
Viewing angle

Constraint
on EOS

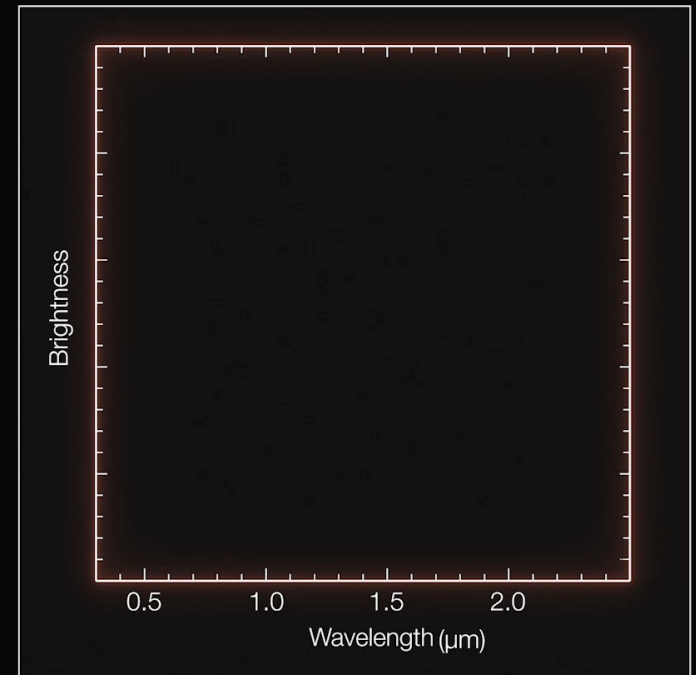
Diagnostic (2) Kilonova

- Excellent agreement with pre-170817 predictions
- High-resolution spectrum, difficult to analyse (need atomic data for highly ionized heavy elements)
- Evidence for high opacity - Two ejectas?
Dynamical (lanthanide-rich, red KN) + Polar (lanthanide-poor, blue)

ESO
(XSHOOTER)



Time: -1225 days



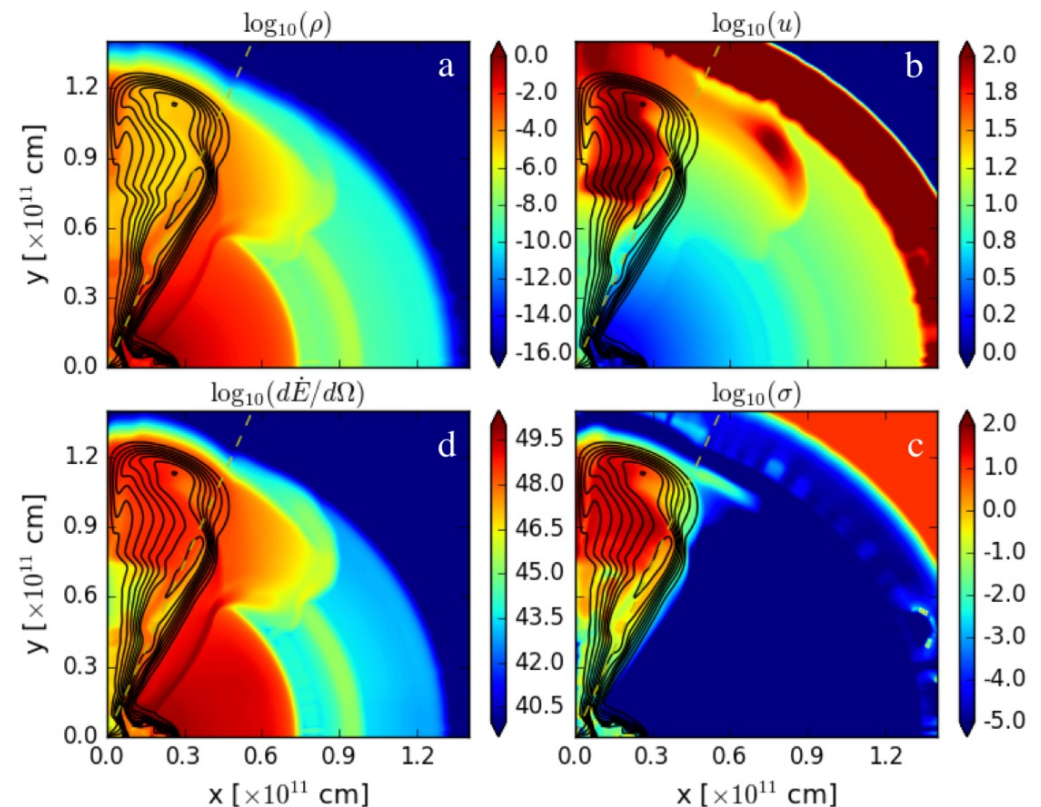
Diagnostic (3) Host galaxy

- NGC 4993
- Lenticular, gas poor
- Offset, low density at the merger location
- Compatible with a merger time of several 100 Myr



Diagnostic (4) Short Gamma-Ray Burst

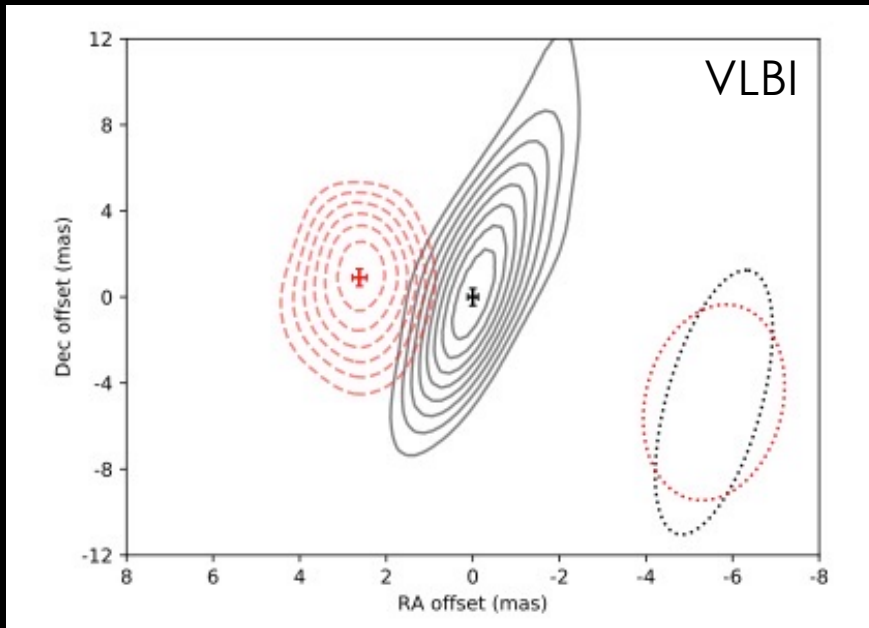
- Very weak
- Ultra-relativistic jet seen very off-axis?**
Probably not ($\gamma\gamma$ opacity argument, Matsumoto+ 19)
- Shock breakout (interaction jet + kilonova ejecta) ?**
see e.g. Bromberg+ 18



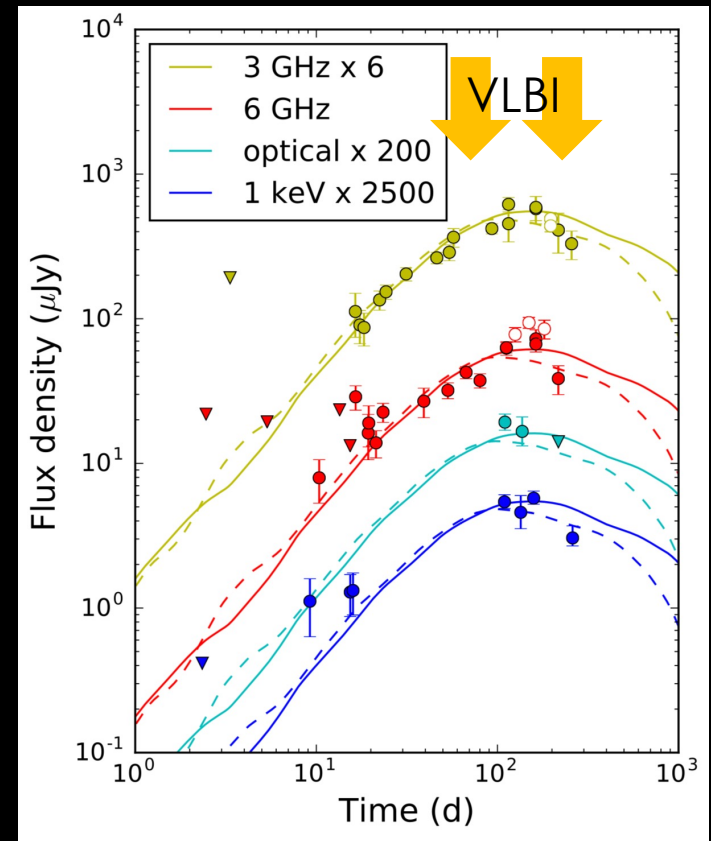
Diagnostic (5) Afterglow

- Photometry: slow rise for more than 100 days, then decay
- VLBI measurements at peak:
 - superluminal apparent motion
 - compact size
- LC: lateral structure (due to jet-KN ejecta interaction?)

Relativistic jet confirmed!



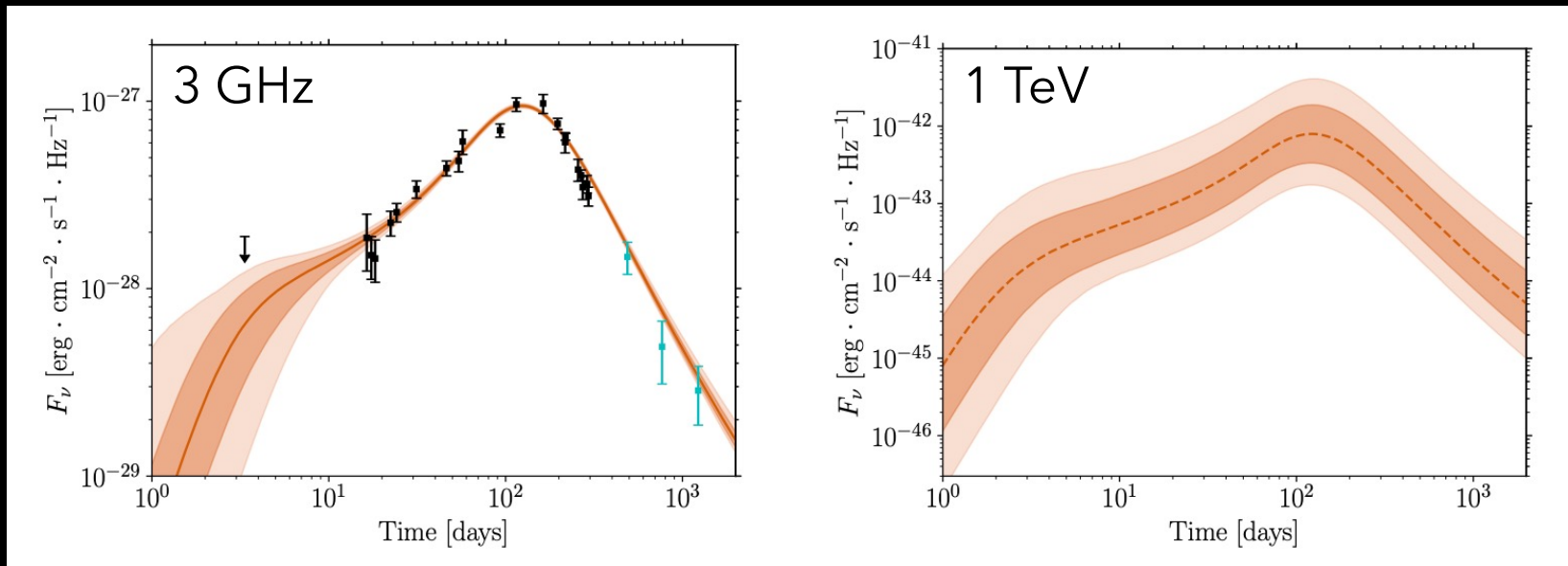
Mooley et al. 2018



Alexander et al. 2018

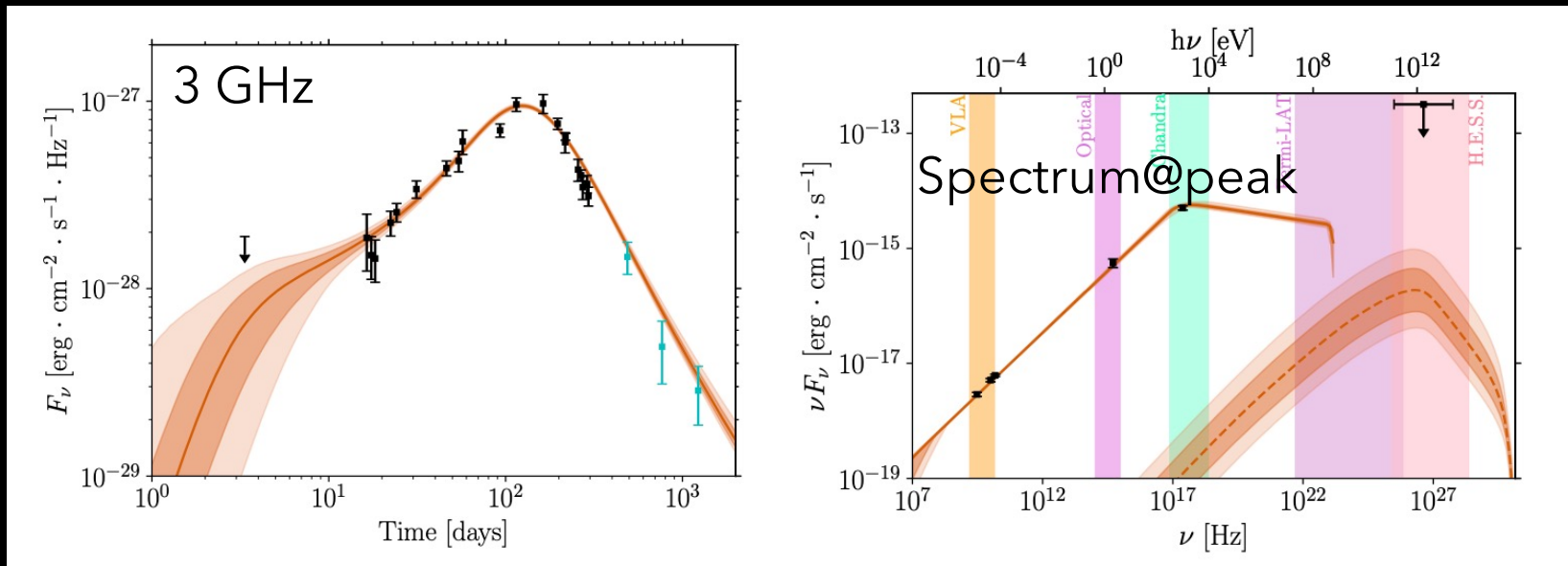
Diagnostic (5) Afterglow

- Best fit:
 - High kinetic energy of the core jet (bright SGRB for an on-axis observer)
 - Good constraint on viewing angle
- Synchrotron component well detected: radio to X-rays
- SSC at VHE?



Diagnostic (5) Afterglow

- Best fit:
 - High kinetic energy of the core jet (bright SGRB for an on-axis observer)
 - Good constraint on viewing angle
- Synchrotron component well detected: radio to X-rays
- SSC at VHE?

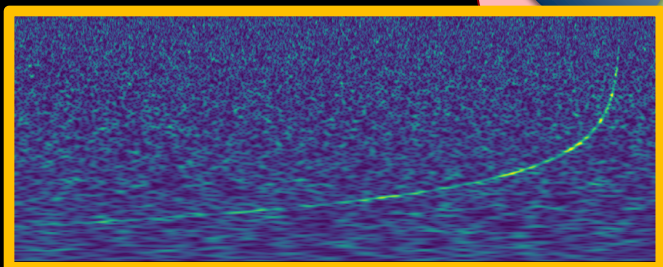
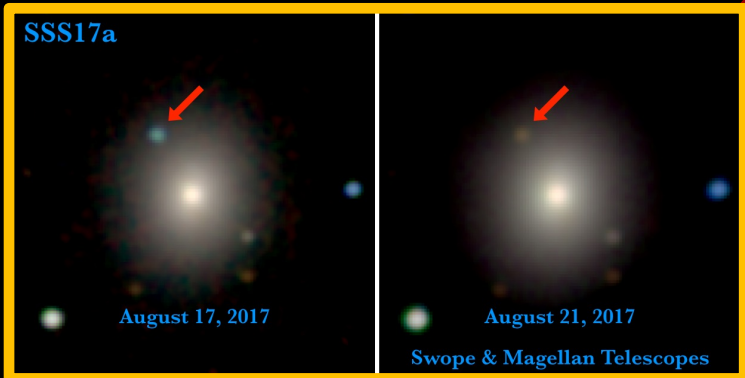


Pellouin & Daigne 2024

Slightly lower view angle + higher external density: detectable by CTA up to 100 Mpc

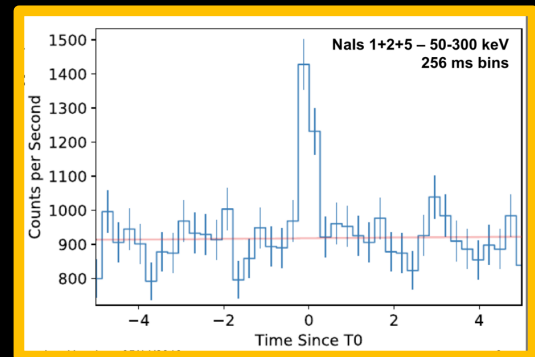
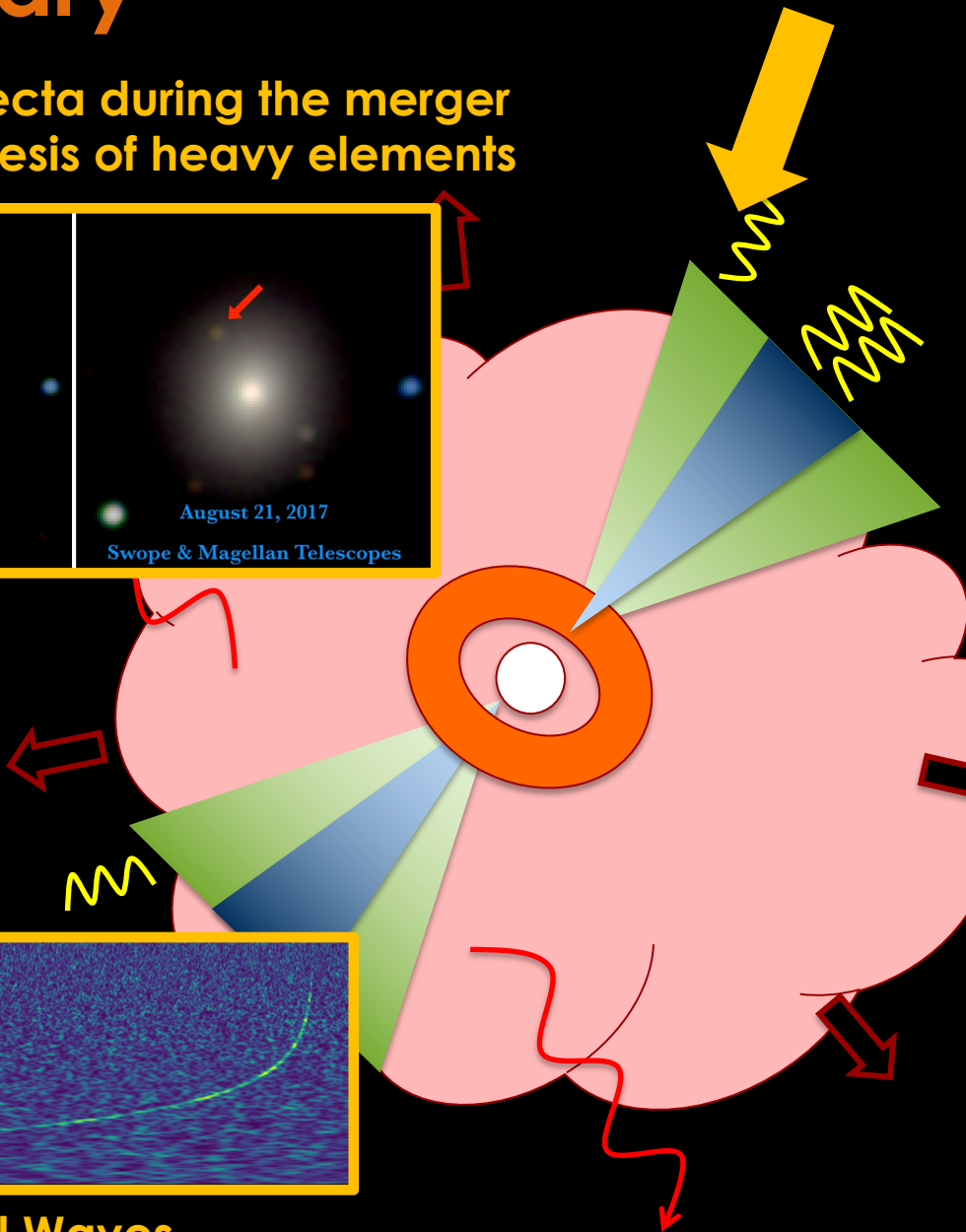
Summary

**Kilonova: ejecta during the merger
Nucleosynthesis of heavy elements**



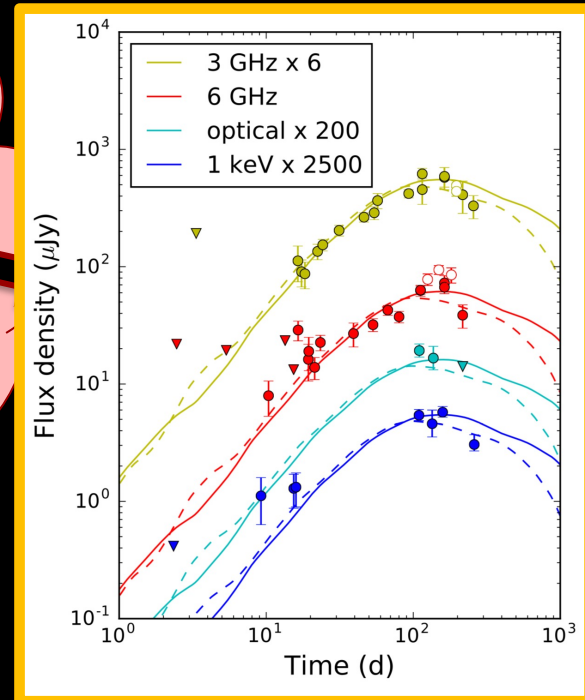
**Gravitational Waves
Inspiral phase of a BNS**

Observer



**Short GRB: relativistic jet
Shock breakout?**

**Bright short GRB
for on-axis observer?**



**Afterglow: deceleration
of a structured relativistic jet**

Fundamental physics: GW+GRB

Fermi



Gamma rays, 50 to 300 keV

GRB 170817A

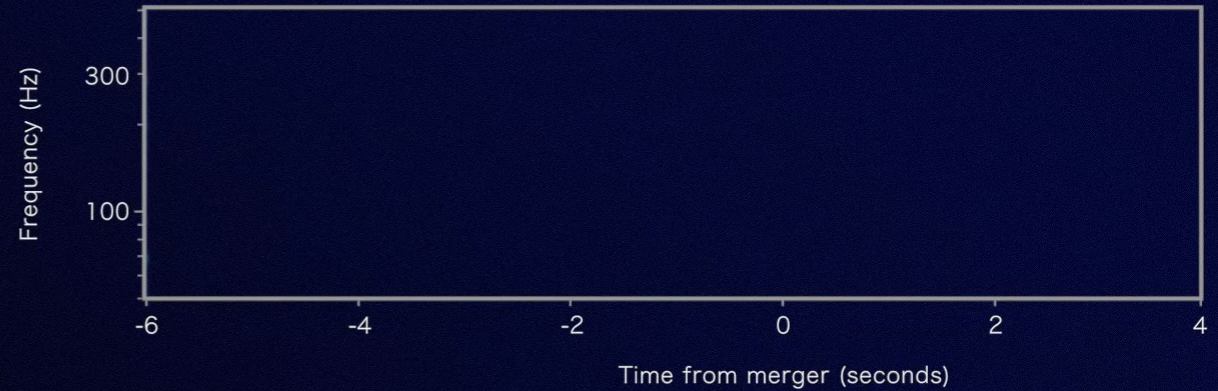


LIGO



Gravitational-wave strain

GW170817



Fundamental physics: GW+GRB

- Delay GW-GRB: max 1.7 s in 130 Myr
Strict limit on the speed of gravitational waves.

$$\frac{c_{\text{GW}} - c}{c} < 10^{-15}$$

Abbott+17 (LV+Fermi paper)

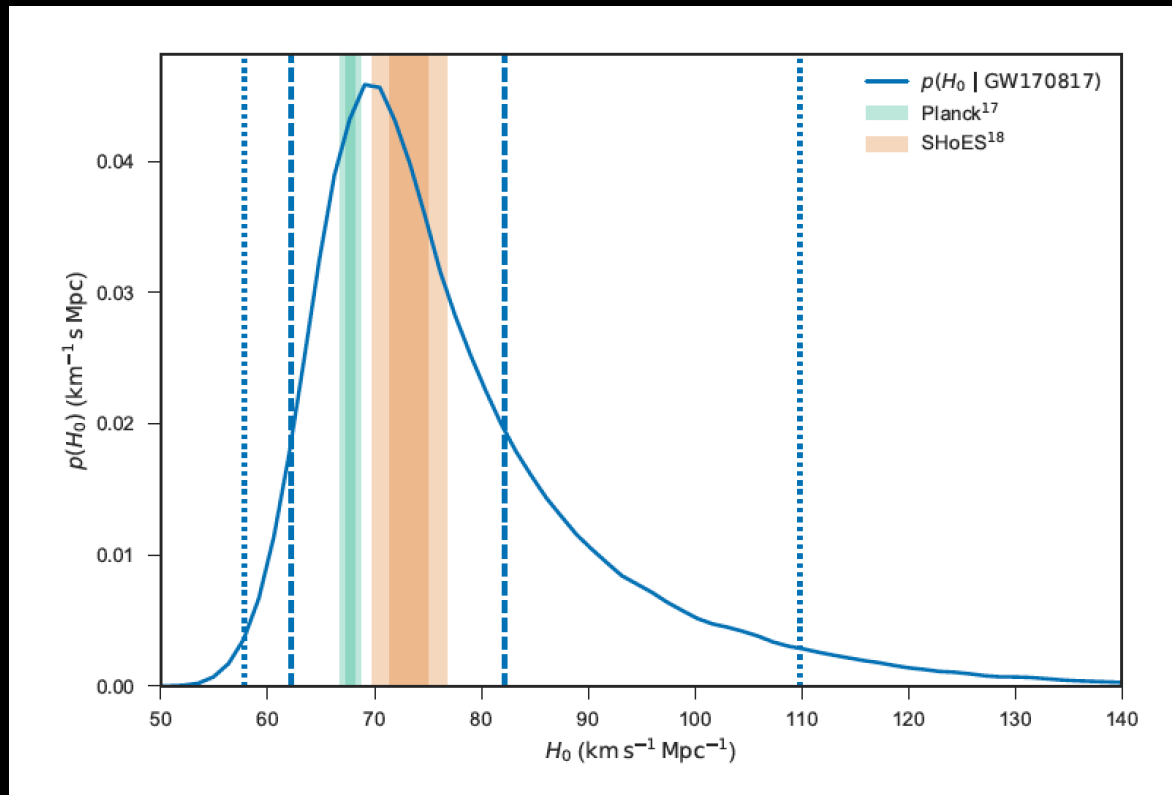
- Astrophys.: delay = delay(merger-relativistic ejection)
+ delay(jet propagation before emiss.)

**Multi-messenger cosmology:
measuring H_0 with
gravitational waves**

GW + host redshift

- GW: distance (uncertainty dominated by D-i degeneracy)
- Host: redshift (low distance: uncertainty for proper motion)

$$H_0 = 70.0_{-8.0}^{+12.0} \text{ km/s/Mpc}$$



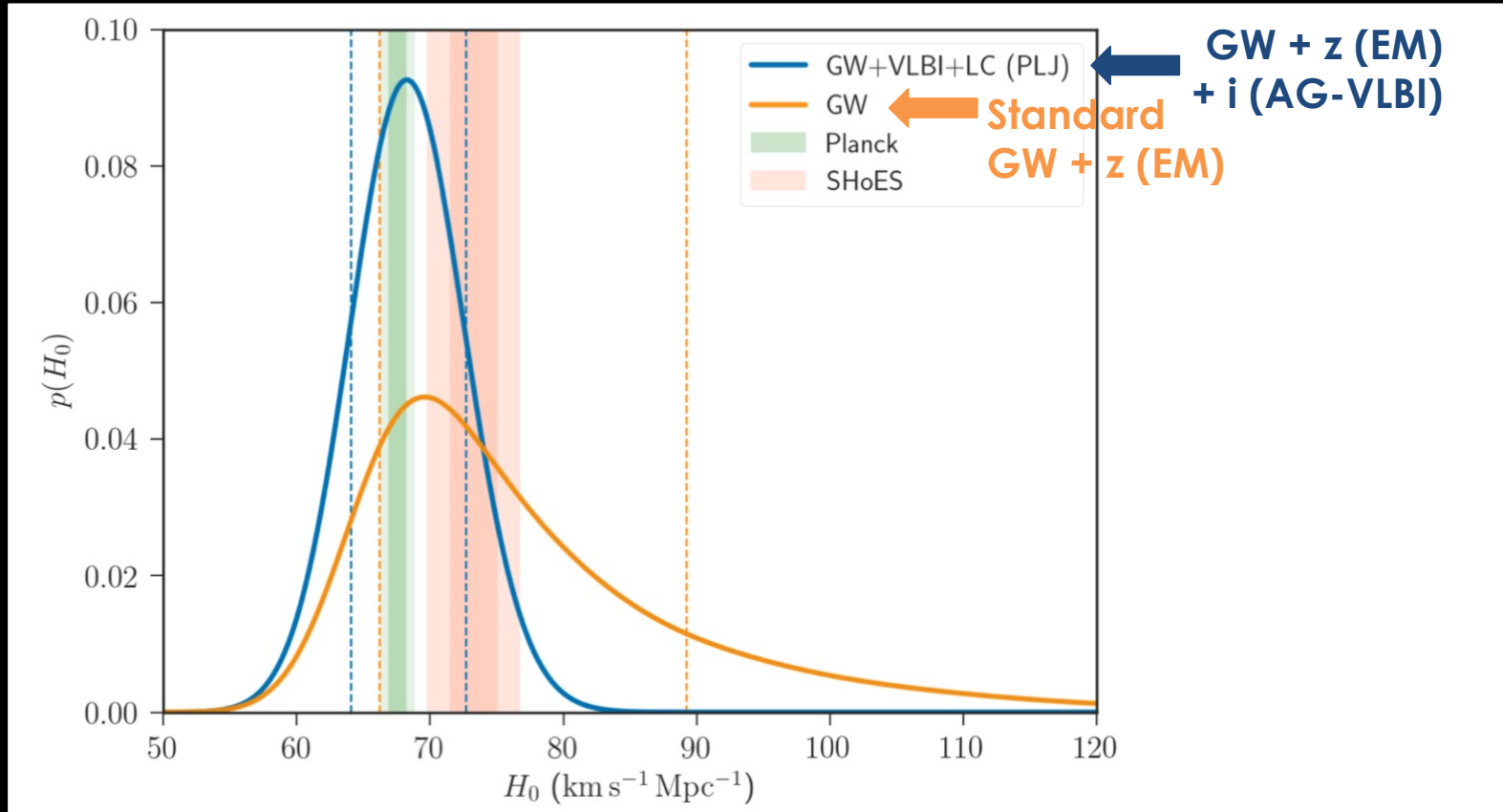
Abbott+17 (H0 paper)

- 2% accuracy? 50-100 GW+optical counterpart MM-events (Chen+ 18)

GW + host redshift + afterglow

- Afterglow with VLBI: constraint on viewing angle

$$H_0 = 70.3^{+5.3}_{-5.0} \text{ km/s/Mpc}$$

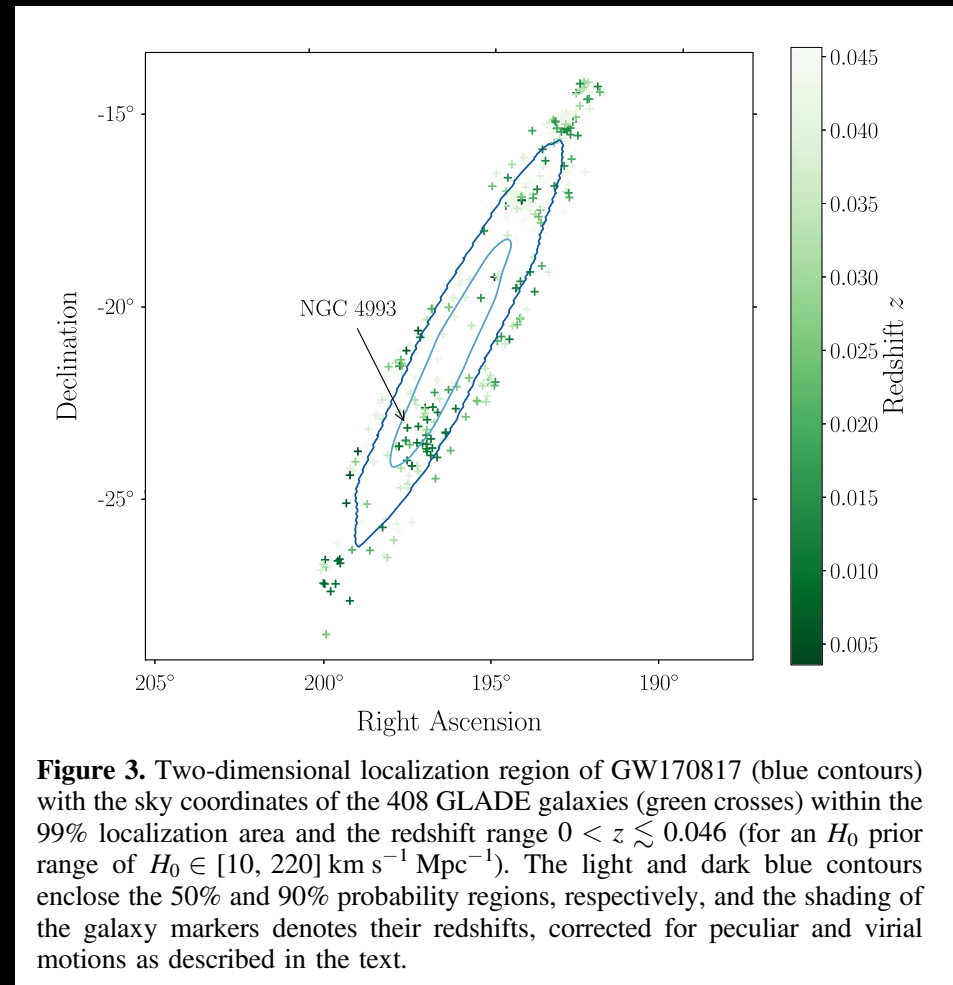


Hotokezaka et al. 2019

Statistical approach

- No em counterpart, GW only + galaxy catalogs
- Redshift averaged over all galaxies in the 3D error box (Schutz 1986)

Application to GW170817

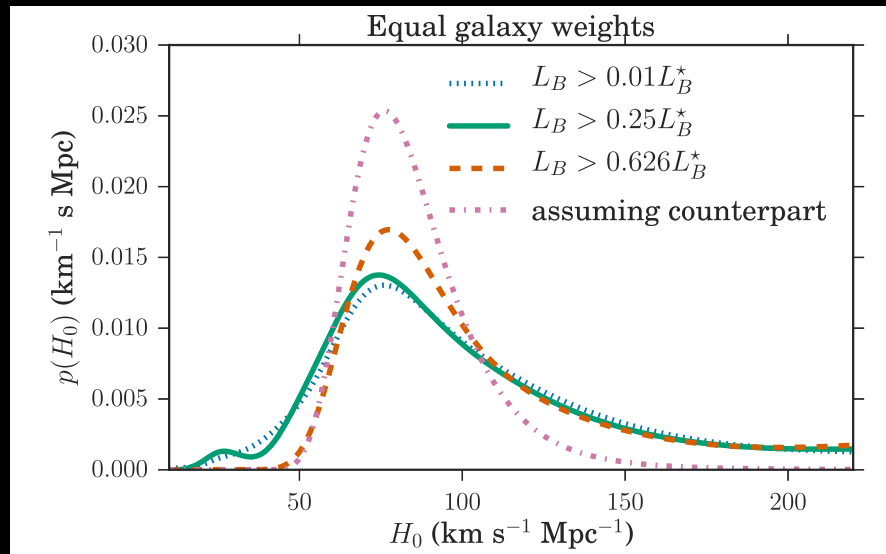


Statistical approach

- Application to 170817: Fishbach +19

$$H_0 = 77_{-18}^{+37} \text{ km s}^{-1} \text{ Mpc}^{-1}$$

- Possible biases:
 - Completeness of galaxy catalogs at large z
 - Are all galaxies equi-probable as hosts?
(complex question, linked to the physics of stellar evolution in binaries)
 - See detailed analysis in Fishbach+19, Gair+22



Fishbach +19

Einstein Telescope

- « Science with the Einstein Telescope: a comparison of different designs », Branchesi+ 23 (arXiv:2303.15923)
ET+Rubin LSST (detections per year)

Full (HFLF cryo) sensitivity detectors

Configuration	$N_{\text{GW,VRO}}$ $\Omega < 20 \text{ deg}^2$	VRO time	$N_{\text{GW,VRO}}$ $\Omega < 40 \text{ deg}^2$	VRO time	$N_{\text{GW,VRO}}$ $\Omega < 100 \text{ deg}^2$	VRO time
$\Delta 10$	14 (14)	1.1% (3.3%)	36 (39)	5.1% (15%)	96	40%
$\Delta 15$	38 (42)	3.3% (9.8%)	84 (101)	14.2% (42%)	163	> 100%
2L 15	28 (28)	2.2% (6.5%)	62 (77)	10.6% (31%)	189	93%
2L 20	55 (64)	5% (14.9%)	115 (152)	23.1% (68%)	324	> 100%

(normalization uncertainty: factor 10)

HF sensitivity detectors

Configuration	$N_{\text{GW,VRO}}$ $\Omega < 20 \text{ deg}^2$	VRO time	$N_{\text{GW,VRO}}$ $\Omega < 40 \text{ deg}^2$	VRO time	$N_{\text{GW,VRO}}$ $\Omega < 100 \text{ deg}^2$	VRO time
$\Delta 10$	0 (0)	0% (0%)	2 (2)	0.3% (0.8%)	4	2%
$\Delta 15$	2 (2)	0.2% (0.5%)	3 (4)	0.7% (1.9%)	8	7.5%
2L 15	3 (4)	0.4% (1.2%)	7 (7)	1.3% (3.9%)	26	11%
2L 20	5 (4)	0.6% (1.6%)	15 (18)	3.1% (9.3%)	32	20.8%

Same without low-frequency

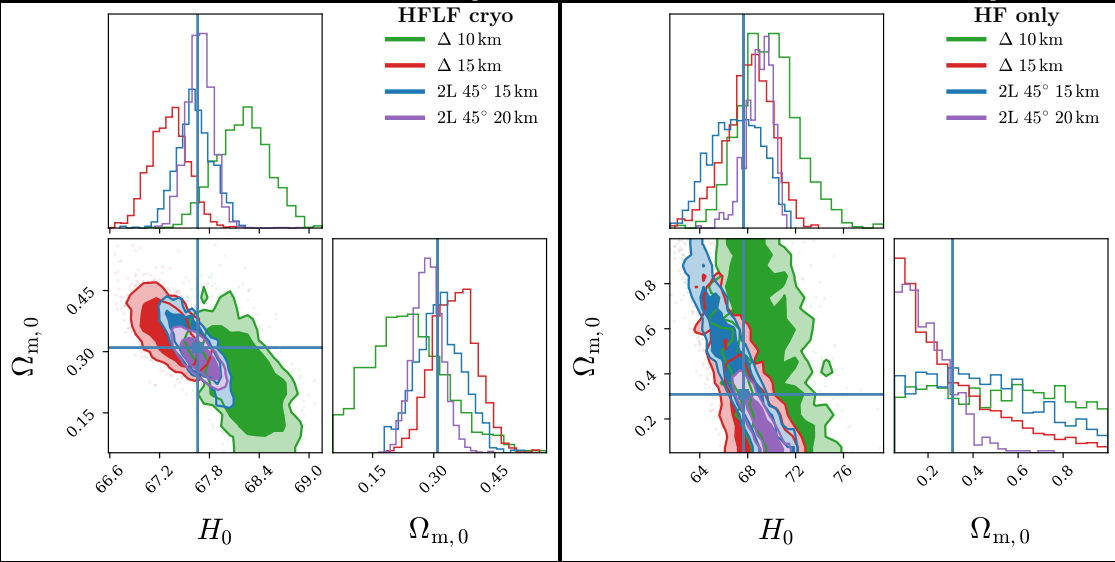
Einstein Telescope

- « Science with the Einstein Telescope: a comparison of different designs », Branchesi+ 23 (arXiv:2303.15923)

ET+Rubin LSST

HFLF cryogenic		
Configuration	$\Delta H_0/H_0$	$\Delta\Omega_M/\Omega_M$
Δ -10km	0.009	0.832
Δ -15km	0.007	0.303
2L-15km-45°	0.006	0.370
2L-20km-45°	0.004	0.243

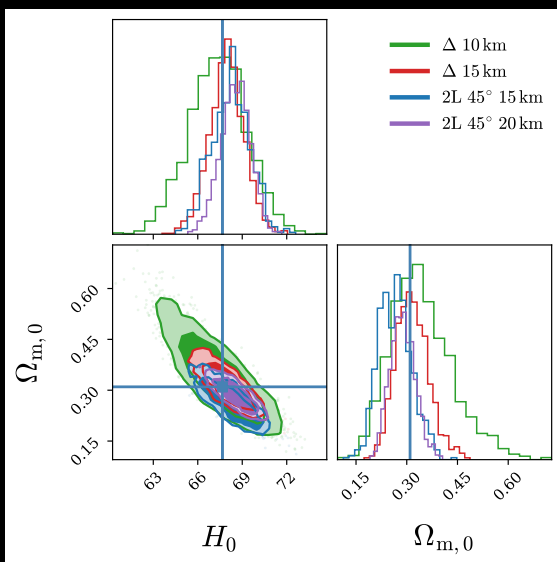
HF only		
Configuration	$\Delta H_0/H_0$	$\Delta\Omega_M/\Omega_M$
Δ -10km	0.065	1.23
Δ -15km	0.057	1.86
2L-15km-45°	0.066	1.31
2L-20km-45°	0.031	1.22



1 yr

ET+THESEUS

Configuration	$\Delta H_0/H_0$	$\Delta\Omega_M/\Omega_M$
Δ -10km	0.057	0.546
Δ -15km	0.035	0.290
2L-15km-45°	0.040	0.370
2L-20km-45°	0.029	0.276



5 yr

Conclusion

Conclusion

- **Multi-Messenger Astrophysics is just starting.**
- **Different messengers carry very complementary physical information**
- **Huge potential in Astrophysics /Cosmology/Fundamental Physics**
- **Very difficult challenge on the instrumental/observational strategy side**
- **We need to exploit all channels**

For example for BNS:

GW + KN ; GW + AG ; GW + GRB
GRB+AG+KN+host
Binary pulsars in the MW

GWB
Orphan KN+host ; Orphan AG+host
etc.